IEEE Access
Multidisciplinary ⋮ Rapid Review ⋮ Open Access Journal

Received 31 March 2023, accepted 25 April 2023, date of publication 2 May 2023, date of current version 10 May 2023.
Digital Object Identifier 10.1109/ACCESS.2023.3272531

RESEARCH ARTICLE

A New Method for the Design of Interval Type-3 Fuzzy Logic Systems With Uncertain Type-2 Non-Singleton Inputs (IT3 NSFLS-2): A Case Study in a Hot Strip Mill

G. M. MENDEZ[1], ISMAEL LOPEZ-JUAREZ[2], P. N. MONTES-DORANTES[3], AND M. A. GARCIA[3]
[1]Electrical and Electronics Engineering Department, Instituto Tecnológico Nacional de México, Campus Nuevo León, Guadalupe, Nuevo León 67170, Mexico
[2]Robotics and Advanced Manufacturing Department, CINVESTAV-IPN Saltillo, Ramos Arizpe, Coahuila 25900, Mexico
[3]Faculty of Physical and Mathematical Sciences, Universidad Autónoma de Nuevo León, San Nicolás de los Garza, Nuevo León 66455, Mexico

Corresponding authors: Ismael Lopez-Juarez (ismael.lopez@cinvestav.edu.mx) and G. M. Mendez (gerardo.m@nuevoleon.tecnm.mx)

This work was supported in part by the Consejo Nacional de Ciencia y Tecnología (CONACyT) under Grant PN-2015-01-1354.

ABSTRACT This paper presents a new method for the construction and training of interval type-3 fuzzy logic systems whose inputs are uncertain type-2 non-singleton numbers (IT3 NSFLS-2). The proposed methodology is divided in two processes: 1) The novel construction of the structure of the IT3 NSFLS-2 systems based on: a) The level-alpha-0 of the interval type-2 fuzzy logic system (IT2-alpha-0 FLS), and on b) The secondary membership function using Gaussian modeling to construct each rule of the alpha-k fuzzy rule base (FRB), the firing intervals of the antecedent and the centroids of the consequent, and 2) The training methodology based on gradient descent algorithm to train the antecedent and consequent parameters of the alpha-0 FRB. The primary membership functions (MF) of the antecedents of the IT3 NSFLS-2 system are modeled as Gaussians with uncertain means and with common standard deviation. The proposal was applied and tested with the prediction of a transfer bar's surface temperature in an industrial hot strip mill facility located in Monterrey México. The modeling results show that the proposal supports the stability required by this critical process and shows the best performance when compared with similar methods.

INDEX TERMS General type-2 fuzzy systems, gradient descent algorithm, hot strip mill, interval type-2 fuzzy systems, interval type-3 fuzzy systems, temperature prediction, type-2 non-singleton inputs.

I. INTRODUCTION

Recent trends on science have generated an evolution of fuzzy systems. This evolution was marked by the development of new models as in the case of the interval type-3 (IT3) fuzzy logic systems (FLS). This type of system was proposed in 2008 by Rickard, et al. with the term type-3 fuzzy sets [1], [2]. I. [3] the IT3 and the type-n systems models were presented in forecasting application.

In recent years, 2019-2022, important and novel papers were developed [4], [5], [6], [7], [8], [9], [10], [11], [12], [13], [14], [15], [16], [17], [18], [19], [20], [21], [22], [23], [24], [25], [26], [27], [28], [29], [30], [31], [32], [33], [34], [35], [36], [37], [38], [39], [40], [41], [42]: Castillo et al. [4], [5], [6], [7], [8], [9], [10], [11], [12], [13], [14], [15], [16], [17], [18], [19], [28], [34], Castillo et al. [4], [5], [6], [8], [9], [10], [11], [12], [13], [14], [18], [19], Castillo et al. [4], [5], [8], [9], [10], [11], [13], [14], [18], Mohammadzadeh et al. [15], [16], [20], [21], [22], [23], [25], [26], [27], [28], [29], [30], [31], [32], [33], [34], [35], [36], [38], [39], [40], [41], [42], among others. Their work shows that the IT3 FLS systems constitute an emerging technology.

In [34, p. 154] the IT3 FLS are defined as:

> "The type-3 FLS, is the generalization of the type-2 FLS that has more capacity to cope with uncertainties. In T3-FLSs, the secondary membership function (MF) is also a type-2 MF. Then the upper and lower bounds of

The associate editor coordinating the review of this manuscript and approving it for publication was Qi Zhou.

memberships are not constant in contrast to the type-2 MFs. These features cause that more level of uncertainties can be handled by type-3 MFs."

The IT3 model presents several similarities to the general type-2 (GT2) model due to their analogous mathematical foundations. The authors in [10] present a list of characteristics for similar intelligent systems as provided in Table 1. It shows that the IT3 FLS provide better accuracy than the IT2 systems.

TABLE 1. Characteristics of the IT3 compared with other models. adapted from [10].

Method	Learning required	Knowledge required	Type of model	Time to develop	Accuracy
NNs	Yes	No	Monolithic	Long	Good
Ensemble NNs	Yes	No	Hybrid	Long	Excellent
ANFIS	Yes	No	Hybrid	Long	Excellent
T1FS	No	Yes	Monolithic	Short	Regular
T2FS	No	Yes	Monolithic	Short	Good
IT3FS	No	Yes	Monolithic	Short	Excellent

Table 2 shows the challenges to be avoided in the implementation of GT2 models as it is mentioned in [43].

TABLE 2. Challenges of the generalization of type-2 fls. adapted from [43].

Challenge	References
Difficult to implement	[44]
Information is non-functional	[45]
Information is un useful	[45]
Information not needed	[45]
Complex learning process	[46-50]
Hard computation	[46, 49-53]
Defuzzification very complex	[46, 53, 54]
Exhaustive computational time	[46, 49-53]
Impractical to usage	[46]
Method iterative and algorithmic	[55]
Determination of the number of alpha planes	[51]

Based on the information above and according to [10] and [43], the main advantages of IT3FS are: a) Superior accuracy versus IT2 models, b) Better system performance, c) Management of non-uniform uncertainties, d) Management of semantically numerical values that the secondary membership function of IT2 cannot make [58]. The disadvantages are: a) Complex learning process due to the change of the type of the secondary membership function, b) Hard computation and their iterative nature, c) Quantity of alpha planes or slices necessary for the implementation and d) Limited number of applications available in the literature.

In [56], [57], and [58] the authors proposed to handle higher levels of uncertainty using IT3 FLS. Nowadays, several researchers have developed its mathematical foundations and applied it to modeling, predicting, and controlling real-world situations.

In [21] the authors presented the baseline to construct and update the IT3 FLS with singleton inputs using a fractional-order learning algorithm, and only the consequent parameters are adjusted to help to decrease the computational cost.

The analysis of the state-of-the-art literature shows that IT3 models use singleton inputs [4], [5], [6], [7], [8], [9], [10], [11], [12], [13], [14], [15], [16], [17], [18], [19], [20], [21], [22], [23], [24], [25], [26], [27], [28], [29], [30], [31], [33], [34], [35], [36], [37], [38], [39], [40], [41], [42] and type-1, non-singleton inputs [32]. The applications of the IT3 FLS systems mainly covers the areas of: Mathematical theory [1], [2], [3], [4], [6], [11], [19], [24], [56], [57], [58], [59], [60], [61], [62], [63], quality of sound and image processing [5], [9], control systems [5], [7], [8], [9], [15], [16], [17], [20], [22], [23], [25], [27], [28], [29], [31], [32], [33], [36], [39], [64], [65], [66], fuzzy learning [16], [20], [21], [26], [27], [34], [36], [40], time series forecasting [3], [10], [13], parameters optimization [8], [26], fault detection [30], [64], [65], stabilization and synchronization [35], [64], management [37], prediction [12], [13], [14], [18], [25], [29], [38], [41], [42], and dynamic adaptation [65], [66]. On the other hand, there exists a gap in the theory and the characteristics, design, and formulation of the involved mathematics of the IT3 models as: the number of rules, the number of alpha planes, and the number of required optimization parameters. All pertinent information respect to the previous characteristics of the systems is omitted in the state-of-the-art literature, as it is shown in Table 3. Also, most of the papers show the particularity of getting the alpha cuts from only one level or only a vector of consequent parameters and from there the alpha cuts or slices are obtained.

In the state-of-the-art literature analysis, there are only few papers that used the gradient descent (GD) method for learning: For instance, authors in [40] use only the pure model and in [34] the extended Kalman filter (EKF) with hybridization is used. The main characteristics of the IT3 FLS found in the state-of-the-art literature are shown in Table 3. It is important to note that most of the publications present only a common vector of 4 or 8 fixed equations for the α_k-cuts calculation in the consequent section (CCS). The use of CCS appears in [7], [15], [20], [21], [22], [24], [28], [30], [34], [35], [41], and [42].

The main contributions of this paper are:

1. An alternative and economical model to construct IT3 NSFLS-2 systems with dynamical structure, where each $2N$ horizontal levels-α_k has its own base of M rules. The output y_{α_k} of each level-α_k is calculated with the contribution of each i^{th} rule, which only requires both its antecedent's firing intervals $\left[\underline{f}^i_{l\alpha_k}, \overline{f}^i_{r\alpha_k}\right]$ and its consequent's centroids $\left[\underline{c}^i_{l\alpha_k}, \overline{c}^i_{r\alpha_k}\right]$. According to the literature, each output y_{α_k} of each level-α_k is calculated using the estimation of the alpha cuts at level-α_k. This proposal does not estimate each α_k-cut of each input x'_q at each level-α_k, that is

TABLE 3. State of art and survey of IT3 systems.

Ref.	Inputs			Learning algorithm		Antecedent & construction Gaussian primary membership function		Structure & output estimation			Simulation	
	S[a]	T1 NS[b]	T2 NS[c]	Antecedent	Consequent	Same mean different standard deviations	Different means same standard deviation	A set of antecedents per horizontal slice	A set of consequents per horizontal slice	Rules M	Horizontal slices K	Number of optimized parameters
[21]	X				Fractional order	X		K vectors of 4 elements per α-cut per input per rule. K = slice levels n = inputs $n = M$ number of rules	CCS Only on level α_k=0	3	4	6
[24]	X			Only the estimation of parameters m and n	Only the estimation of parameters m and n	X		ρ vectors of 4 elements per α-cut per input per rule. ρ = slice levels and ρ = inputs M = number of rules	CCS	3,4,5, 6	6	2
[30]		X		Maximum correntropy (MC) unscented Kalman filter (UKF)	Maximum (MC) unscented Kalman filter (UKF)	X		η vectors of 4 elements per α-cuts per input per rule. η = slice levels τ = inputs N =number of rules	CCS	No	No	No
[40]		X		Gradient descent (GD)	Gradient descent (GD)	X		$n = h$ = vectors of 4 elements per α-cut per input per rule. $n = h = 4$ = slice levels = number of rules 2 = inputs	$n = h$ = vectors of 4 elements (α-cuts) per input per rule.	4	4	16
[34]		X		Gradient descent (GD) + extended Kalman filter (EKF)	UKF	X		$n = h$ = vectors of 4 elements per α-cut per input per rule. $n = h = 8$ = slice levels 3 = inputs R = number of rules	CCS	8	8	No
[22]		X		Specific adaptation rules using derivatives.	Specific adaptation rules using derivatives.	X		$n = h$ = vectors of 4 elements per α-cuts per input per rule. $n = h = 8$ = slice levels 2 = inputs R = number of rules	CCS	Not shown	Not shown	Not shown
[28]	X			Unscented Kalman filter (CUKF)	CUKF	X		h = vectors of 4 elements per α-cut per input per rule. h = slice levels n = inputs $\beta = n_r$ number of rules	CCS	Not shown	Not shown	Not shown
[35]	X			Specific control law	Specific control law	X		h = vectors of 4 equations per α-cut per input per rule. $\nu_l = 3$ = slice levels $n = 3$ inputs r = number of rules	CCS	Not shown	Not shown	Not shown
[10]		X				X		n = inputs m = output n = number of rules	n clusters $C_1, \ldots, C_n$	6	3	Not shown
[7]	X			Differential evolution (DE)		X			CCS	9	Not shown	10
[15]	X			Specific adaptation law	Specific adaptation law	X		h = vectors of 4 equations per α-cut per input per rule. m = inputs n_α = number of level-α $l = R$ = rules i = outputs	CCS	3	$n_\alpha = 3$ $\underline{\alpha}$ = [0,0.25,0.5] $\overline{\alpha}$ = [0.75,0.90,1.0]	
[20]		X		Upper bound of approximate error (AE)		X		h = vectors of 8 equations per α-cut per input per rule. m = inputs n_α = number of level-α $l = R = 8$ rules $\hat{f} = 2$ outputs	CCS	8	Not shown	Not shown
[41]	X				UKF	X		h = vectors of 4 equations per α-cut per input per rule. ι = number of level-α $M = 8$ rules	CCS	10	4	Not shown
[42]		X		Fractional order		X		h = vectors of 4 equations per α-cut per input per rule.	CCS	Not shown	2 $\underline{\alpha}$ = [0.85,0.95] $\overline{\alpha}$ = [0.90,1.0]	Not shown

TABLE 3. ***(Continued.)*** **State of art and survey of IT3 systems.**

Our proposal	X	GD	GD	$M_q^i \in [M_{q_1}^i, M_{q_2}^i]$ = interval means σ_q^i = common standard deviation	$R = i$ = rules = firing intervals per level-α $\left[\underline{f}_{l\alpha_k}^i, \overline{f}_{r\alpha_k}^i\right]$ k = number of level-α	$R = i$ = rules = Consequent centroids per level-α $\left[\underline{c}_{l\alpha_k}^i, \overline{c}_{r\alpha_k}^i\right]$ k = number of level-α	25	1,10,100, and 1000	11 parameters per rule 25x11= 275

[a] Singleton, [b] Type-1 non-singleton, [c] Type-2 non-singleton.

$\left[a_{q\alpha_k}^i\left(x_q'\right), b_{q\alpha_k}^i\left(x_q'\right)\right]$, in order to calculate the firing interval values $\left[\underline{f}_{l\alpha_k}^i, \overline{f}_{r\alpha_k}^i\right]$ of this level-α_k.

2. The use of Gaussian models to directly calculate the firing interval $\left[\underline{f}_{l\alpha_k}^i, \overline{f}_{r\alpha_k}^i\right]$ of each fuzzy rule at each level-α_k using for the basis of this estimation the firing interval of the level-α_0, $\left[\underline{f}_{l\alpha_o}^i, \overline{f}_{r\alpha_o}^i\right]$.
3. The use of two sets of product operations required to calculate the values of the α_k-cuts for each input variable, of each rule at each level-α_k. e.g. If an IT3 NSFLS-2 fuzzy system has $p = 2$ input variables x_1', x_2', $M = 25$ rules, and $K = 20$ levels-α_k, then the new proposal does not require the calculation of (24) and (25) for a total of 2000 α_k-cuts $= 2pMK = 2 \times 2 \times 25 \times 20$ times, for each estimation of y_α.
4. To the best knowledge of the authors, this is the first time that the primary MFs of the antecedents section of the IT3 NSFLS-2 are modeled as Gaussians with uncertain mean $M_q^i \in \left[M_{q1}^i, M_{q2}^i\right]$ and common standard deviation σ_q^i, Fig. 1, with such being a more difficult case than the one considered in the state-of-the-art literature that uses the primary MFs modeled as Gaussians with uncertain standard deviation $\sigma_q^i \in \left[\sigma_{q1}^i, \sigma_{q2}^i\right]$ and a common mean M_q^i.
5. The proposal handles the type-2 non-singleton inputs modeled as Gaussians fuzzy numbers with uncertain standard deviations $\sigma_{x_q}^i \in \left[\sigma_{x_{q1}}^i, \sigma_{x_{q2}}^i\right]$, representing the additive measurement non-stationary noise (Fig. 1). An interval type-3 FLS whose inputs are modeled using type-2 fuzzy numbers is named a type-2 non-singleton type-3 fuzzy logic system (IT3 NSFLS-2).
6. The complete set of equations to update all the parameters of both antecedent and consequent sections of the proposed dynamical structure which are obtained by applying the gradient descent methodology, is presented here.
7. To the best of the knowledge of the authors, this is the first time that the IT3 NSFLS-2 fuzzy systems are applied to predict the transfer bar surface temperature at the entry zone of the finishing scale breaker of a hot strip mill.
8. To the best knowledge of the authors, this is the first time that systematic experiments using IT3 NSFLS-2 fuzzy systems with more than 10 levels-α_k are proposed: 100 and 1000 levels-α_k.

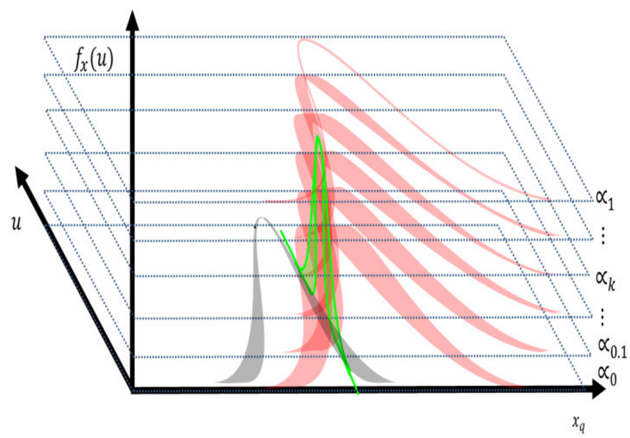

FIGURE 1. **Levels-α and uncertain secondary values of the proposed IT3 NSFLS-2 system.**

II. PROBLEM DESCRIPTION

The Hot Strip Mill (HSM) process presents many complexities and uncertainties involved in rolling operations. Fig. 2 shows the HSM sub-processes: The reheat furnace, the roughing mill (RM), the transfer tables, the scale breaker (SB), the finishing mill (FM), the round out tables, and the coiler (CLR).

The most critical subprocess is the FM. There are several mathematical model-based systems for setting up the FM, like the finishing mill setup (FSU) model which calculates the working references required to obtain the target strip gauge, target strip width and target strip temperature at the exit zone of the FM. The FSU model takes as inputs the FM target strip gage, the target strip width, the target strip temperature, the slab steel grade, the hardness ratio from slab chemistry, the FM load distribution, the FM gauge offset, the FM temperature offset, the FM roll diameters, the FM load distribution, the input transfer bar gauge, the input transfer bar width, and the most critical variable, the input transfer bar temperature.

The FSU model requires knowing accurately what the input transfer bar temperature is at the entry zone of the FM. A minimum entry temperature error will propagate through the entire FM and produce a coil out of the required quality. For the estimation of this FM entry temperature, the math models require knowledge of the transfer bar surface

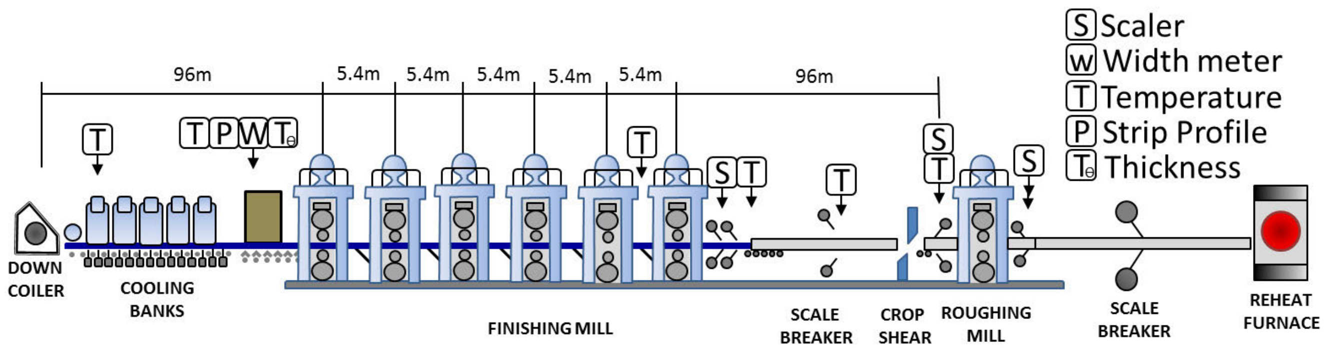

FIGURE 2. Topology of a typical HSM.

temperature, which is measured by a pyrometer located at the RM exit side, and the time taken to translate the transfer bar from the RM exit zone to the FM SB entry zone.

These pyrometers' measurements are affected by the noise produced by the surface scale growth, environment water steam, the pyrometer's location, calibration, resolution, repeatability, and by the recalescence phenomenon occurring at the RM exit in the body of the transfer bar [67]. The time required by the transfer bar to move its head end from the RM exit to the FM entry zones, is estimated by the FSU model, when calculating the required transfer bar thread speed to reach the strip target temperature at the exit zone of the FM. This time estimation is affected by the free air radiation phenomenon occurring during the transfer bar translation and by the inherent uncertainty of the kinematic and dynamic modeling.

The FSU model parameters are adjusted using both, the uncertain surface temperature measured by pyrometers located at the FM entry zone, and the uncertain surface temperature at the FM entry zone estimated by the FSU model. The proposal was off-line tested using real data from an industrial hot strip mill facility located in Monterrey, México, which is currently using a certain type of fuzzy system for this estimation.

III. CONSTRUCTION OF THE IT3 NSFLS-2

The main foundation of IT3 systems is the uncertainty presented by the horizontal level-α_k with respect to its vertical location or its secondary membership value $\mu_{\tilde{A}}(x,u) = f_x(u) = \alpha_k$, as is shown in Fig. 1. In the IT3 systems, this additional uncertainty is represented by the interval value $[\underline{\alpha}_k, \overline{\alpha}_k]$. Geometrically as in [21], it is interpreted as shown in Fig. 3. This uncertainty is modeled to be between the horizontal level $\underline{\alpha}_k$ and the horizontal level $\overline{\alpha}_k$, as in Fig. 4.

Based on the economical modeling of WH GT2 Mamdani fuzzy systems that use the type reduction center sets and the end-point defuzzification average [60], [61], [62], [63], the IT3 NSFLS-2 can be calculated as in [60], with $q = 1, 2, \ldots, p$ the number of input variables, $i = 1, 2, \ldots, 2M$ the number of rules, $k = 1, 2, \ldots, N$, and the number of

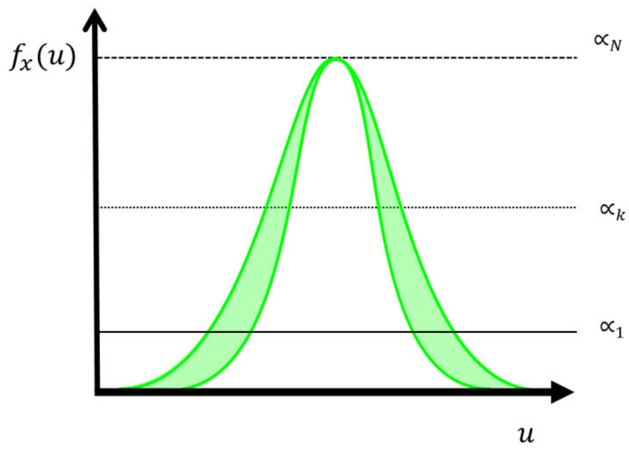

FIGURE 3. Uncertainty of secondary membership grade in IT3 system.

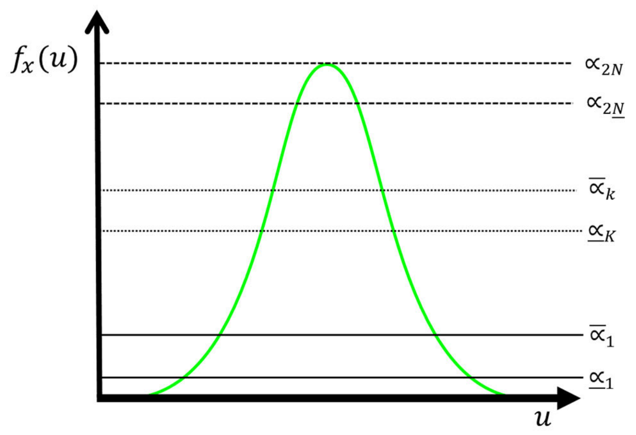

FIGURE 4. Uncertainty of secondary membership grade in GT2 equivalent to IT3 systems.

initial horizontal levels-α_k:

$$f_{IT3NSFLS-2}\left(\boldsymbol{x}'\right) = y_{WH-3} = y_{\alpha} = \frac{\sum_{k=1}^{k_{max}} \alpha_k y_{\alpha_k}}{\sum_{k=1}^{k_{max}} \alpha_k} \tag{1}$$

$$y_{\alpha_k} = \left[\frac{y_{l\alpha_k} + y_{r\alpha_k}}{2}\right] \tag{2}$$

$$f_{IT3NSFLS-2}(x') = y_{WH-3} = y_\alpha = \frac{\sum_{k=1}^{k_{max}} \alpha_k \left[\left(y_{l,\alpha_k}^{cos}(x') + y_{r,\alpha_k}^{cos}(x')\right)/2\right]}{\sum_{k=1}^{k_{max}} \alpha_k} \tag{3}$$

where y_{l,α_k}^{cos} and y_{r,α_k}^{cos} are the left and right points of the center of sets of each y_{α_k}, and its union can be expressed as an expansion y_{WH-3} composed by N elements y_{α_k} corresponding to the N horizontal levels-α_k:

$$y_\alpha = \frac{\alpha_1}{\sum_{n=0}^{N}\alpha_n} y_{\alpha_1} + \frac{\alpha_2}{\sum_{n=0}^{N}\alpha_n} y_{\alpha_2} + \ldots + \frac{\alpha_k}{\sum_{n=0}^{N}\alpha_n} y_{\alpha_k} + \ldots + \frac{\alpha_N}{\sum_{n=0}^{N}\alpha_n} y_{\alpha_N} \tag{4}$$

Each weighted output y_{α_k} corresponding to each level α_k can be calculated using the IT3 NFLS-2 modeling with the uncertain level $\alpha_k \in \left[\underline{\alpha}_k, \overline{\alpha}_k\right]$. Now the proposed y_{WH-3} expansion is composed by $2N$ elements, as in Fig. 4.

$$y_\alpha = \frac{\alpha_1}{\sum_{n=0}^{N}\alpha_n}\left(\frac{\underline{\alpha}_1 y_{\underline{\alpha}_1} + \overline{\alpha}_1 y_{\overline{\alpha}_1}}{\underline{\alpha}_1 + \overline{\alpha}_1}\right) + \ldots + \frac{\alpha_k}{\sum_{n=0}^{N}\alpha_n}\left(\frac{\underline{\alpha}_k y_{\underline{\alpha}_k} + \overline{\alpha}_k y_{\overline{\alpha}_k}}{\underline{\alpha}_k + \overline{\alpha}_k}\right) + \ldots + \frac{\alpha_N}{\sum_{n=0}^{N}\alpha_n}\left(\frac{\underline{\alpha}_N y_{\underline{\alpha}_N} + \overline{\alpha}_N y_{\overline{\alpha}_N}}{\underline{\alpha}_N + \overline{\alpha}_N}\right) \tag{5}$$

$$y_\alpha = \frac{\alpha_1}{\sum_{n=0}^{N}\alpha_n}\left(\frac{\underline{\alpha}_1 y_{\underline{\alpha}_1}}{\underline{\alpha}_1 + \overline{\alpha}_1}\right) + \frac{\alpha_1}{\sum_{n=0}^{N}\alpha_n}\left(\frac{\overline{\alpha}_1 y_{\overline{\alpha}_1}}{\underline{\alpha}_1 + \overline{\alpha}_1}\right) + \ldots + \frac{\alpha_k}{\sum_{n=0}^{N}\alpha_n}\left(\frac{\underline{\alpha}_k y_{\underline{\alpha}_k}}{\underline{\alpha}_k + \overline{\alpha}_k}\right) + \frac{\alpha_k}{\sum_{n=0}^{N}\alpha_n}\left(\frac{\overline{\alpha}_k y_{\overline{\alpha}_k}}{\underline{\alpha}_k + \overline{\alpha}_k}\right) + \ldots + \frac{\alpha_N}{\sum_{n=0}^{N}\alpha_n}\left(\frac{\underline{\alpha}_N y_{\underline{\alpha}_N}}{\underline{\alpha}_N + \overline{\alpha}_N}\right) + \frac{\alpha_N}{\sum_{n=0}^{N}\alpha_n}\left(\frac{\overline{\alpha}_N y_{\overline{\alpha}_N}}{\underline{\alpha}_N + \overline{\alpha}_N}\right) \tag{6}$$

$$y_\alpha = K_{\underline{\alpha}_1} y_{\underline{\alpha}_1} + K_{\overline{\alpha}_1} y_{\overline{\alpha}_1} + \ldots + K_{\underline{\alpha}_k} y_{\underline{\alpha}_k} + K_{\overline{\alpha}_k} y_{\overline{\alpha}_k} + \ldots + K_{\underline{\alpha}_N} y_{\underline{\alpha}_N} + K_{\overline{\alpha}_N} y_{\overline{\alpha}_N} \tag{7}$$

$$y_\alpha = K_{\alpha_1} y_{\alpha_1} + K_{\alpha_2} y_{\alpha_2} + \ldots K_{\alpha_k} y_{\alpha_k} + \ldots + K_{\alpha_N} y_{\alpha_N} + K_{\alpha_{N+1}} y_{\alpha_{N+1}} + \ldots + K_{\alpha_{2N-1}} y_{\alpha_{2N-1}} + K_{\alpha_{2N}} y_{\alpha_{2N}} \tag{8}$$

Now y_α of the IT3 NSFLS-2 can be modeled as any GT2 NSFLS-2 system as it is shown in Fig. 4.
where

$$K_{\alpha_1} = \frac{\alpha_1}{\sum_{n=0}^{N}\alpha_n}\left[\frac{\underline{\alpha}_1}{\underline{\alpha}_1 + \overline{\alpha}_1}\right] \tag{9}$$

$$K_{\alpha_2} = \frac{\alpha_1}{\sum_{n=0}^{N}\alpha_n}\left[\frac{\overline{\alpha}_1}{\underline{\alpha}_1 + \overline{\alpha}_1}\right] \tag{10}$$

$$\vdots$$

$$K_{\alpha_k} = \frac{\alpha_k}{\sum_{n=0}^{N}\alpha_n}\left[\frac{\underline{\alpha}_k}{\underline{\alpha}_k + \overline{\alpha}_k}\right] \tag{11}$$

$$K_{\alpha_{k+1}} = \frac{\alpha_k}{\sum_{n=0}^{N}\alpha_n}\left[\frac{\overline{\alpha}_k}{\underline{\alpha}_k + \overline{\alpha}_k}\right] \tag{12}$$

$$\vdots$$

$$K_{\alpha_{2N-1}} = \frac{\alpha_{2N-1}}{\sum_{n=0}^{N}\alpha_n}\left[\frac{\underline{\alpha}_N}{\underline{\alpha}_N + \overline{\alpha}_N}\right] \tag{13}$$

$$K_{\alpha_{2N}} = \frac{\alpha_{2N}}{\sum_{n=0}^{N}\alpha_n}\left[\frac{\overline{\alpha}_N}{\underline{\alpha}_N + \overline{\alpha}_N}\right] \tag{14}$$

then:

$$y_\alpha = K_{\alpha_1}\left[\frac{y_{l\underline{\alpha}_1} + y_{r\underline{\alpha}_1}}{2}\right] + K_{\alpha_2}\left[\frac{y_{l\overline{\alpha}_2} + y_{r\overline{\alpha}_2}}{2}\right] + \ldots + K_{\alpha_k}\left[\frac{y_{l\underline{\alpha}_k} + y_{r\underline{\alpha}_k}}{2}\right] + K_{\alpha_{k+1}}\left[\frac{y_{l\overline{\alpha}_{k+1}} + y_{r\overline{\alpha}_{k+1}}}{2}\right] + \ldots + K_{\alpha_{2N-1}}\left[\frac{y_{l\underline{\alpha}_{2N-1}} + y_{r\underline{\alpha}_{2N-1}}}{2}\right] + K_{\alpha_{2N}}\left[\frac{y_{l\overline{\alpha}_{2N}} + y_{r\overline{\alpha}_{2N}}}{2}\right] \tag{15}$$

$$y_\alpha = \sum_{k=1}^{2N} K_{\alpha_k}\left[\frac{y_{l\alpha_k} + y_{r\alpha_k}}{2}\right] \tag{16}$$

The centroids can be calculated with the centroid equations using the Karnik-Mendel (KM) algorithm for any left endpoint $y_{l\alpha_k}$:

$$y_{l\alpha_k} = \frac{\sum_{n=1}^{L}\overline{f}_{\alpha_k}^{n} * c_{l\alpha_k}^{n} + \sum_{n=L+1}^{M}\underline{f}_{\alpha_k}^{n} * c_{l\alpha_k}^{n}}{\sum_{n=1}^{L}\overline{f}_{\alpha_k}^{n} + \sum_{n=L+1}^{M}\underline{f}_{\alpha_k}^{n}} \tag{17}$$

and for any right endpoint $y_{r\alpha_k}$:

$$y_{r\alpha_k} = \frac{\sum_{n=1}^{R}\underline{f}_{\alpha_k}^{n} * c_{r\alpha_k}^{n} + \sum_{n=R+1}^{M}\overline{f}_{\alpha_k}^{n} * c_{r\alpha_k}^{n}}{\sum_{n=1}^{R}\underline{f}_{\alpha_k}^{n} * + \sum_{n=R+1}^{M}\overline{f}_{\alpha_k}^{n}} \tag{18}$$

$\left[\underline{f}_{\alpha_k}^{n}, \overline{f}_{\alpha_k}^{n}\right]$ is the estimated firing interval and $\left[c_{l\alpha_k}^{n}, c_{r\alpha_k}^{n}\right]$ is the estimated consequent centroid of the rule n of the level-α_k.

A. INPUT VARIABLES, RULES, AND LEVELS-α_k

The designer must select $q = 1, 2, \ldots, p$ the input variables, $i = 1, 2, \ldots, M$ the number of rules, $k = 1, 2, \ldots, N$, the initial number of horizontal levels-α_k to start the construction of the IT3 NSFLS-2 system.

The p inputs are type-2 non-singleton numbers modeled as a Gaussian with common mean x_q' and an interval of standard deviations $\sigma_{\tilde{X}_q} \in \left[\sigma_{X_{q1}}, \sigma_{X_{q2}}\right]$. The well-known type-2 non-singleton Gaussian model [61 and 68] is used as primary MF:

$$\mu_{\tilde{X}_q}(x_q) = exp\left[-\frac{1}{2}\left[\frac{x_q - x_q'}{\sigma_{x_{q_k}}}\right]^2\right] \tag{19}$$

Each input must cover its universe of discourse (UOD) with the required number of MF.

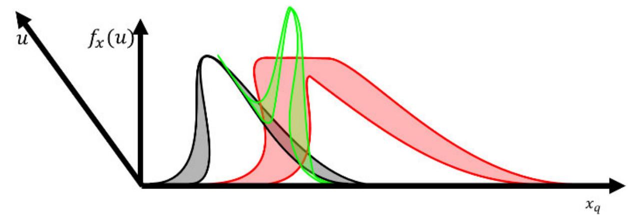

FIGURE 5. Graphic representation of the proposed model, the IT3 NSFLS-2 system.

B. UNIVERSE OF DISCOURSE AND MF

The number M of rules is determined by the array of required MFs of each input. If there are two inputs, and the UOD of $\tilde{X}_1$ and $\tilde{X}_2$ are covered by five MFs each, then the rule base has $M = 5 \times 5 = 25$ rules.

As it is shown in Fig. 5, each consequent MF is modeled as Gaussian with uncertain means $M_q^i \in \left[M_{q1}^i, M_{q2}^i\right]$ and common standard deviation σ_q^i:

$$\mu_{\tilde{A}_q^i}(x_q) = exp\left[-\frac{1}{2}\left[\frac{x_q - M_q^i}{\sigma_q^i}\right]^2\right] \tag{20}$$

The GT2 Mamdani fuzzy rule base model has p inputs $x_1 \in X_1, \ldots, x_p \in X_p$, one output $\in Y$, and a rule base of size M of the form:

$$\tilde{R}^i : IF\ x_1\ is\ \tilde{A}_1^i\ and\ \ldots and\ x_q\ is\ \tilde{A}_q^i\ THEN\ y\ i.\ \tilde{G}^i \tag{21}$$

where $q = 1, 2, \ldots, p$ is the number of inputs; $i = 1, 2, \ldots, M$ is the number of rules.

C. RULE BASE

The rule base of the horizontal level-α_0 of M rules, is constructed assigning the initial values of each of the M consequent centroids $\left[\underline{c}_{l\alpha_0}^i, \overline{c}_{r\alpha_0}^i\right]$. These values can be fixed by an expert or with initialization fixed at zero.

$$\tilde{R}^i : IF\ x_1\ i.\ \tilde{A}_1^i\ and\ \ldots x_q\ i.\ \tilde{A}_q^i\ THEN\ y\ is\ \left[\underline{c}_{l\alpha_0}^i, \overline{c}_{r\alpha_0}^i\right] \tag{22}$$

D. ALPHA CUTS

The M firing intervals $\left[\underline{f}_{l\alpha_0}^i, \overline{f}_{r\alpha_0}^i\right]$ of the horizontal level-α_0 or IT2α_0 FLS are calculated based on (23) using the α_0-cuts or the intersection of x_q' and the MF of each input and each rule. Only the α_0-cuts of level-α_0 are calculated, not the α_k-cuts of any other level-α_k, as shown in Table 3.

$$\left[\underline{f}_{l\alpha_0}^i, \overline{f}_{r\alpha_0}^i\right] = \left[\prod_{q=1}^{p} a_{q\alpha_0}^i\left(\underline{x}_{q,max}^i\right), \prod_{q=1}^{p} b_{q\alpha_0}^i\left(\overline{x}_{q,max}^i\right)\right] \tag{23}$$

with

$$a_{q\alpha_0}^i\left(\underline{x}_{q,max}^i\right) = \underline{\mu}_{\tilde{X}_q}(\underline{x}_{q,max}^i)\underline{\mu}_{\tilde{A}_q^i}(\underline{x}_{q,max}^i) \tag{24}$$

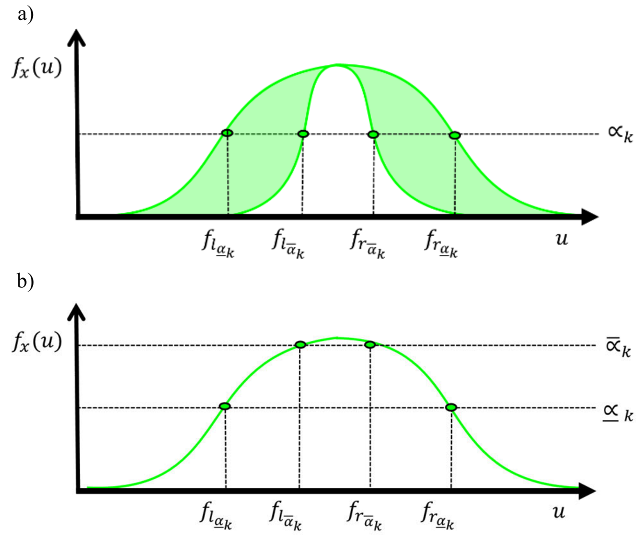

FIGURE 6. Geometrical view used to calculate, a) For each level-α_k, each α_k-cut point of the firing interval of the antecedent section of the proposed IT3 NSFLS-2 systems, and b) Its equivalent geometrical view in GT2 systems.

and

$$b_{q\alpha_0}^i\left(\overline{x}_{q,max}^i\right) = \overline{\mu}_{\tilde{X}_q}(\overline{x}_{q,max}^i)\overline{\mu}_{\tilde{A}_q^i}(\overline{x}_{q,max}^i) \tag{25}$$

$\underline{x}_{q,max}^i$ and $\overline{x}_{q,max}^i$ are determined according to the locations of x_q' with respect to M_{q1}^i and M_{q2}^i as it is shown in Table 4.

E. FIRING INTERVALS

Each firing interval $\left[\underline{f}_{l\alpha_0}^i, \overline{f}_{r\alpha_0}^i\right]$ of the horizontal level-α_0 or IT2α_0 NSFLS-2 is used to estimate the antecedent's firing interval at each level-$\alpha_k \in \left[\underline{\alpha}_k, \overline{\alpha}_k\right]$. As it is shown in Fig. 6, the Gaussian model of the vertical slice at $x_{q,max}'$ used to calculate the firing interval $\left[\underline{f}_{l\alpha_k}^i, \overline{f}_{r\alpha_k}^i\right]$ of each level-α_k is:

$$\mu_{f_{vs\alpha_k}^i} = \alpha_k = exp\left[-\frac{1}{2}\left[\frac{x_q' - m_{fvs\alpha_0}^i}{\sigma_{fvs\alpha_0}^i}\right]^2\right] \tag{26}$$

where

$$m_{f_{vs\alpha_0}}^i = \frac{\underline{f}_{l\alpha_0}^i + \overline{f}_{r\alpha_0}^i}{2} \tag{27}$$

$$\sigma_{f_{vs\alpha_0}}^i = \frac{\overline{f}_{r\alpha_0}^i - \underline{f}_{l\alpha_0}^i}{Z} \tag{28}$$

$$\left[\underline{f}_{l\alpha_k}^i, \overline{f}_{r\alpha_k}^i\right] = \frac{\underline{f}_{l\alpha_0}^i + \overline{f}_{r\alpha_0}^i}{2} \mp \frac{\overline{f}_{r\alpha_0}^i - \underline{f}_{l\alpha_0}^i}{Z}\sqrt[2]{-2\ln(\alpha_k)} \tag{29}$$

with $z = 1, 2, \ldots, n$ being an integer number estimated by trial and error. The magnitude of the standard deviation of the model is a fraction of the interval of the means.

F. CONSEQUENT CENTROIDS

Each consequent's centroids $\left[\underline{c}_{l\alpha_0}^i, \overline{c}_{r\alpha_0}^i\right]$ of the horizontal level-α_0 are used to estimate the consequents' centroid of the

TABLE 4. Locations of x'_q, for $x^i_{low_q}$ and $x^i_{up_q}$ estimation used to calculate $\left[\underline{f}^i_{l\alpha_0}, \overline{f}^i_{r\alpha_0}\right]$ and $\left[\underline{f}^i_{l\alpha_k}, \overline{f}^i_{r\alpha_k}\right]$.

Case	Location of x'_q for $\underline{x}^i_{q,max}$ calculation	Location of x'_q for $\overline{x}^i_{q,max}$ calculation	$\underline{x}^i_{q,max}$	$\overline{x}^i_{q,max}$
1	$x'_q < \frac{M^i_{q1\alpha_0}+M^i_{q2\alpha_0}}{2} - \frac{\left(\sigma^i_{x_{q1}}\right)^2\left(M^i_{q2\alpha_0}-M^i_{q1\alpha_0}\right)}{2\left(\sigma^i_{q\alpha_0}\right)^2}$	$x'_q < M^i_{q1\alpha_0}$	$\underline{x}^i_{q,max} = \frac{\left(\sigma^i_{x_{q1}}\right)^2 M^i_{q2\alpha_0} + \left(\sigma^i_q\right)^2 x'_q}{\left(\sigma^i_{x_{q1}}\right)^2 + \left(\sigma^i_{q\alpha_0}\right)^2}$	$\overline{x}^i_{q,max} = \frac{\left(\sigma^i_{x_{q2}}\right)^2 M^i_{q1\alpha_0} + \left(\sigma^i_q\right)^2 x'_q}{\left(\sigma^i_{x_{q2}}\right)^2 + \left(\sigma^i_{q\alpha_0}\right)^2}$
2	$x'_q < \frac{M^i_{q1\alpha_0}+M^i_{q2\alpha_0}}{2} - \frac{\left(\sigma^i_{x_{q1}}\right)^2\left(M^i_{q2\alpha_0}-M^i_{q1\alpha_0}\right)}{2\left(\sigma^i_{q\alpha_0}\right)^2}$	$x'_q \in \left[M^i_{q1\alpha_0}, M^i_{q2\alpha_0}\right]$	$\underline{x}^i_{q,max} = \frac{\left(\sigma^i_{x_{q1}}\right)^2 M^i_{q2\alpha_0} + \left(\sigma^i_q\right)^2 x'_q}{\left(\sigma^i_{x_{q1}}\right)^2 + \left(\sigma^i_{q\alpha_0}\right)^2}$	$\overline{x}^i_{q,max} = x'_q$
3	$x'_q \in \left[\frac{M^i_{q1\alpha_0}+M^i_{q2\alpha_0}}{2} - \frac{\left(\sigma^i_{x_{q1}}\right)^2\left(M^i_{q2\alpha_0}-M^i_{q1\alpha_0}\right)}{2\left(\sigma^i_{q\alpha_0}\right)^2}, \frac{M^i_{q1\alpha_0}+M^i_{q2\alpha_0}}{2} + \frac{\left(\sigma^i_{x_{q1}}\right)^2\left(M^i_{q2\alpha_0}-M^i_{q1\alpha_0}\right)}{2\left(\sigma^i_{q\alpha_0}\right)^2}\right]$	$x'_q \in \left[M^i_{q1\alpha_0}, M^i_{q2\alpha_0}\right]$	$x^i_{low_q} = \frac{M^i_{q1\alpha_0}+M^i_{q2\alpha_0}}{2}$	$\overline{x}^i_{q,max} = x'_q$
4	$x'_q > \frac{M^i_{q1\alpha_0}+M^i_{q2\alpha_0}}{2} + \frac{\left(\sigma^i_{x_{q1}}\right)^2\left(M^i_{q2\alpha_0}-M^i_{q1\alpha_0}\right)}{2\left(\sigma^i_{q\alpha_0}\right)^2}$	$x'_q \in \left[M^i_{q1\alpha_0}, M^i_{q2\alpha_0}\right]$	$\underline{x}^i_{q,max} = \frac{\left(\sigma^i_{x_{q1}}\right)^2 M^i_{q1\alpha_0} + \left(\sigma^i_q\right)^2 x'_q}{\left(\sigma^i_{x_{q1}}\right)^2 + \left(\sigma^i_{q\alpha_0}\right)^2}$	$\overline{x}^i_{q,max} = x'_q$
5	$x'_q > \frac{M^i_{q1\alpha_0}+M^i_{q2\alpha_0}}{2} + \frac{\left(\sigma^i_{x_{q1}}\right)^2\left(M^i_{q2\alpha_0}-M^i_{q1\alpha_0}\right)}{2\left(\sigma^i_{q\alpha_0}\right)^2}$	$x'_q > M^i_{q2}$	$\underline{x}^i_{q,max} = \frac{\left(\sigma^i_{x_{q1}}\right)^2 M^i_{q1\alpha_0} + \left(\sigma^i_q\right)^2 x'_q}{\left(\sigma^i_{x_{q1}}\right)^2 + \left(\sigma^i_{q\alpha_0}\right)^2}$	$\overline{x}^i_{q,max} = \frac{\left(\sigma^i_{x_{q2}}\right)^2 M^i_{q2\alpha_0} + \left(\sigma^i_q\right)^2 x'_q}{\left(\sigma^i_{x_{q2}}\right)^2 + \left(\sigma^i_{q\alpha_0}\right)^2}$

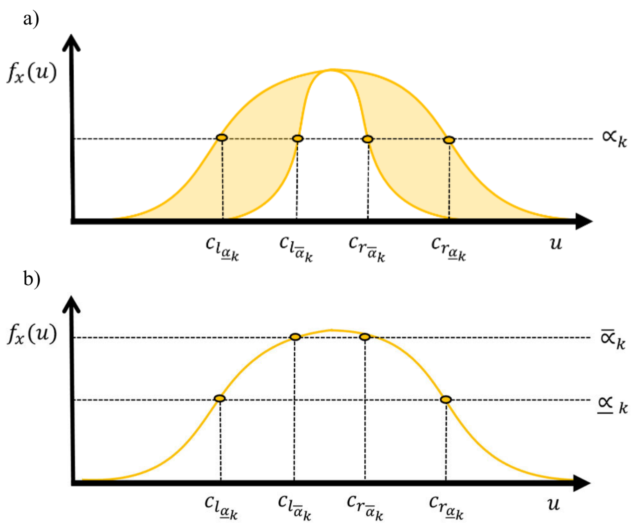

FIGURE 7. Geometrical view used to calculate, a) For each level-α_k, each α_k-cut point of the Centroids of the consequent section of the proposed IT3 NSFLS-2 system, and b) its equivalent geometrical view in GT2 systems.

level-$\alpha_k \in \left[\underline{\alpha}_k, \overline{\alpha}_k\right]$. As shown in Fig. 7, the Gaussian model of the vertical slice at $x'_{q,max}$ used to calculate the centroid $\left[\underline{c}^i_{l\alpha_k}, \overline{c}^i_{r\alpha_k}\right]$ of each level-α_k is:

$$\mu_{c^i_{vs\alpha_k}} = \alpha_k = exp\left[-\frac{1}{2}\left[\frac{x'_q - m^i_{cvs\alpha_0}}{\sigma^i_{cvs\alpha_0}}\right]^2\right] \tag{30}$$

where

$$m^i_{cvs\alpha_0} = \frac{\underline{c}^i_{l\alpha_0} + \overline{c}^i_{r\alpha_0}}{2} \tag{31}$$

$$\sigma^i_{fvs\alpha_0} = \frac{\overline{c}^i_{r\alpha_0} - \underline{c}^i_{l\alpha_0}}{Z} \tag{32}$$

$$\left[\underline{c}^i_{l\alpha_k}, \overline{c}^i_{r\alpha_k}\right] = \frac{\underline{c}^i_{l\alpha_0} + \overline{c}^i_{r\alpha_0}}{2} \mp \frac{\overline{c}^i_{r\alpha_0} - \underline{c}^i_{l\alpha_0}}{Z}\sqrt[2]{-2\ln(\alpha_k)} \tag{33}$$

G. EXPANSION OF THE LEVEL-α_k

The proposed IT3 NSFLS-2 solves the processing of the uncertainty of the secondary grade of each level-α_k, Fig. 3, by replacing this level by its two levels-α_k that represent the uncertainty in the secondary membership: The lower level-$\underline{\alpha}_k$ and the upper level-$\overline{\alpha}_k$. Now the expanded number of the horizontal levels-α_k is $2N$, transforming the IT3 NSFLS-2 into a GT2 NSFLS-2 system, Fig. 4, by applying the WH GT2 methodology to $2N$ levels-α_k (8).

H. CALCULATION OF $\mathbf{y}_\alpha$

For each input-output training data pair $(\boldsymbol{x}', y)$, y_α can be estimated using (16). The proposed IT3 NSFLS-2 is dynamically constructed because its structure is calculated for each input vector $\boldsymbol{x}'_q$. The horizontal level-α_0 or IT2α_0 NSFLS-2 is used as the base line to estimate the structure of each horizontal level-α_k or IT2α_k. Regardless of it being either the low horizontal level-$\underline{\alpha}_k$ or the upper horizontal level-$\overline{\alpha}_k$, it requires the same procedure: In each level-α_k an IT2α_k NSFLS-2 is constructed with its corresponding antecedent firing interval $\left[\underline{f}^i_{l\alpha_k}, \overline{f}^i_{r\alpha_k}\right]$ and its corresponding consequent centroid $\left[\underline{c}^i_{l\alpha_k}, \overline{c}^i_{r\alpha_k}\right]$. An important characteristic is that the estimated parameters of the antecedent and consequent sections of each rule of all the levels-$\alpha_k \in \left[\underline{\alpha}_k, \overline{\alpha}_k\right]$ are dynamic and temporal, and only the parameters of the level-α_0 or IT2α_0 are permanent. Only the level-α_0 has MF parameters of its Gaussians models, while any other level-α_k temporarily has the corresponding estimated firing intervals $\left[\underline{f}^i_{l\alpha_k}, \overline{f}^i_{r\alpha_k}\right]$ and the estimated centroids $\left[\underline{c}^i_{l\alpha_k}, \overline{c}^i_{r\alpha_k}\right]$ both required to calculate its weighted contribution to the y_α final value.

IV. TRAINING ALGORITHM

An objective function $E(\theta)$ may have a non-linear form with respect to an adjustable parameter θ. In the interactive descent methods, the next point $\theta\,(new)$ is determined by one step down from the current point $\theta\,(now)$ in the negative direction of the gradient of the function $E(\theta_{now})$. The K learning rates are selected by trial and error while meeting the selected criteria of minimizing the error.

$$\theta\,(\text{new}) = \theta\,(now) - Kg \tag{34}$$

$$\theta\,(new) = \theta\,(now) - K\frac{\partial E}{\partial \theta_{now}} \tag{35}$$

K is the training rate, and g is the vector of the first partial derivatives of $E(\theta)$ and is equivalent to $\frac{\partial E}{\partial \theta_{now}}$:

$$g(\theta) = \left[\frac{\partial E}{\partial \theta_{1now}}, \frac{\partial E}{\partial \theta_{2now}}, \ldots, \frac{\partial E}{\partial \theta_{nnow}}\right]^T \tag{36}$$

Each rule of the level-α_0 uses (35) to update three θ antecedent parameters, $M^i_{q1\alpha_0}$ (37), $M^i_{q2\alpha_0}$ (38), and $\sigma^i_{q\alpha_0}$ (39), and two θ consequent parameters, $\underline{c}^i_{l\alpha_0}$ (40), and $\overline{c}^i_{r\alpha_0}$ (41).

Equation (35) requires finding the partial derivatives used to update all the parameters of the antecedent and consequent sections of each rule of only the IT2α_0 NFLS-2 located at level-α_0.

$$M^i_{q1\alpha_0}\,(new) = M^i_{q1\alpha_0}\,(now) - K_{M_{q1\alpha_0}}\frac{\partial E}{\partial M^i_{q1\alpha_0}} \tag{37}$$

$$M^i_{q2\alpha_0}\,(new) = M^i_{q2\alpha_0}\,(now) - K_{M_{q2\alpha_0}}\frac{\partial E}{\partial M^i_{q2\alpha_0}} \tag{38}$$

$$\sigma^i_{q\alpha_0}\,(new) = \sigma^i_{q\alpha_0}\,(now) - K_{\sigma_q\alpha_0}\frac{\partial E}{\partial \sigma^i_{q\alpha_0}} \tag{39}$$

$$\underline{c}^i_{l\alpha_0}\,(new) = \underline{c}^i_{l\alpha_0}\,(now) - K_{\underline{c}_l\alpha_0}\frac{\partial E}{\partial \underline{c}^i_{l\alpha_0}} \tag{40}$$

$$\overline{c}^i_{r\alpha_0}\,(new) = \overline{c}^i_{r\alpha_0}\,(now) - K_{\overline{c}_r\alpha_0}\frac{\partial E}{\partial \overline{c}^i_{r\alpha_0}} \tag{41}$$

where $K_{M_{q1\alpha_0}}, K_{M_{q2\alpha_0}}, K_{\sigma_q\alpha_0}, K_{\underline{c}_l\alpha_0}$, and $K_{\overline{c}_r\alpha_0}$ are the training rates of its corresponding parameter.

The quadratic error function to minimize is:

$$E = \frac{1}{2}(y - y_\alpha)^2 \tag{42}$$

where: y is the output value of the L input-output data pairs. The error function is:

$$e = y - y_\alpha \tag{43}$$

As an example, the logic sequence of the math steps to obtain the partial derivatives of the objective function E with respect to the antecedent parameter $M^i_{q1\alpha_0}$ are illustrated from (44) to (46).

$$M^i_{q1\alpha_0}\,(new) = M^i_{q1\alpha_0}\,(now) - K_{M_{q1\alpha_0}}\frac{\partial E}{\partial M^i_{q1\alpha_0}} \tag{44}$$

then

$$\begin{aligned}\frac{\partial E}{\partial M^i_{q1\alpha_0}} = \Bigg[&\frac{\partial E}{\partial y_\alpha}\frac{\partial y_\alpha}{\partial y_{\underline{\alpha}_1}}\frac{\partial y_{\underline{\alpha}_1}}{\partial M^i_{q1\alpha_0}} + \frac{\partial E}{\partial y_\alpha}\frac{\partial y_\alpha}{\partial y_{\overline{\alpha}_1}}\frac{\partial y_{\overline{\alpha}_1}}{\partial M^i_{q1\alpha_0}}\\ &+ \ldots + \frac{\partial E}{\partial y_\alpha}\frac{\partial y_\alpha}{\partial y_{\underline{\alpha}_k}}\frac{\partial y_{\underline{\alpha}_k}}{\partial M^i_{q1\alpha_0}} + \frac{\partial E}{\partial y_\alpha}\frac{\partial y_\alpha}{\partial y_{\overline{\alpha}_k}}\frac{\partial y_{\overline{\alpha}_k}}{\partial M^i_{q1\alpha_0}}\\ &+ \ldots + \frac{\partial E}{\partial y_\alpha}\frac{\partial y_\alpha}{\partial y_{\underline{\alpha}_N}}\frac{\partial y_{\underline{\alpha}_N}}{\partial M^i_{q1\alpha_0}} + \frac{\partial E}{\partial y_\alpha}\frac{\partial y_\alpha}{\partial y_{\overline{\alpha}_N}}\frac{\partial y_{\overline{\alpha}_N}}{\partial M^i_{q1\alpha_0}}\Bigg]\end{aligned} \tag{45}$$

which is equivalent to:

$$\begin{aligned}&\frac{\partial E}{\partial M^i_{q1\alpha_0}}\\ &= \Bigg[\frac{\partial E}{\partial y_\alpha}\frac{\partial y_\alpha}{\partial y_{\alpha_1}}\frac{\partial y_{\alpha_1}}{\partial M^i_{q1\alpha_0}} + \frac{\partial E}{\partial y_\alpha}\frac{\partial y_\alpha}{\partial y_{\alpha_2}}\frac{\partial y_{\alpha_2}}{\partial M^i_{q1\alpha_0}}\\ &+ \ldots + \frac{\partial E}{\partial y_\alpha}\frac{\partial y_\alpha}{\partial y_{\alpha_k}}\frac{\partial y_{\alpha_k}}{\partial M^i_{q1\alpha_0}} + \ldots + \frac{\partial E}{\partial y_\alpha}\frac{\partial y_\alpha}{\partial y_{\alpha_N}}\frac{\partial y_{\alpha_N}}{\partial M^i_{q1\alpha_0}}\\ &+ \ldots \frac{\partial E}{\partial y_\alpha}\frac{\partial y_\alpha}{\partial y_{\alpha_{2N}}}\frac{\partial y_{\alpha_{2N}}}{\partial M^i_{q1\alpha_0}}\Bigg]\end{aligned} \tag{46}$$

Each level-$\alpha_k \in \left[\underline{\alpha}_k, \overline{\alpha}_k\right]$ previously defined during the construction process, contributes only by updating the parameters of the permanent level-α_0. No parameters of the level-α_k have training only have it the level-α_0 parameters.

A similar procedure can be used to calculate the equations for training: $M^i_{q2\alpha_0}$, $\sigma^i_{q\alpha_0}$, $\underline{c}^i_{l\alpha_0}$, and $\overline{c}^i_{r\alpha_0}$ of the IT2α_0 NSFLS-2.

As shown in Table 4, the final equations for training the parameters of the antecedent and the consequent depend on the relative position of x'_q with respect to $M^i_{q1\alpha_0}$ and $M^i_{q2\alpha_0}$ positions. Table 5 shows the complete set of equations for parameters $M^i_{q1\alpha_0}$, $M^i_{q2\alpha_0}$ and $\sigma^i_{q\alpha_0}$, with training under y_l contribution. Table 6 also shows the complete set of equations for training these three antecedent parameters under y_r contribution. Tables 7 and 8 show the equations for training $\underline{c}^i_{l\alpha_0}$ and $\overline{c}^i_{r\alpha_0}$ consequent parameters by adding the contribution of each horizontal level-α_k.

V. CONVERGENCE ANALISYS

The fuzzy-logic identification approach works for the trajectory tracking for a conventional dynamic system. The HSM is a complex system with a complex mathematical description. The objective is to design an IT3 NSFLS-2 identifier to achieve that the output of the fuzzy model converges to the output of the real system as $t \to \infty$, without any knowledge of the plant except the assumptions that its inputs and outputs are measured by sensors and its values are bounded by the limits of the process operation. In [69] and [70] it is established that, by choosing a $\sigma^i_{q\alpha_0}$ as small as σ^*_q the fuzzy system can match all the L input-output data pairs $(\boldsymbol{x}', y)$ to an arbitrary accuracy.

Lemma 1: For arbitrary $\epsilon > 0$, the fuzzy system $f_{IT3NSFLS-2}(\boldsymbol{x}')$ with the initial parameters $M^i_q \in \left[M^i_{q_1}, M^i_{q_2}\right]$ and common standard deviation $\sigma^i_q = \sigma^*_q$, has the property that $\left|f_{IT3NSFLS-2}\left(\boldsymbol{x}'^{(t)}\right) - y^{(t)}\right| < \epsilon$ where $f_{IT3NSFLS-2}(\boldsymbol{x}')$ is the output y_α in the training phase, $\boldsymbol{x}'^{(t)}$ is the input training vector, $y^{(t)}$ is the output training value, with $t = 1, 2, \ldots, L$.

Because the proposed IT3 NSFLS-2 is a universal fuzzy identifier, the training algorithm based on gradient descent guarantees that the total error from (43) converges to a value ϵ at every step of training. This can be proved using the general results of the gradient descent algorithm as defined in [69] and applied to the proposed IT3 NSFLS-2 training.

Let $[\underline{\mathbf{f}}]$ and $\left[\overline{\mathbf{f}}\right]$ be a sequence of real-valued vectors generated respectively by one of the gradient-descent algorithms:

$$\underline{f}\,(new) = \underline{f}\,(now) - \eta\nabla g(\underline{f}\,(now))$$
$$\overline{f}\,(new) = \overline{f}\,(now) - \eta\nabla g(\overline{f}\,(now))$$

where η is the training rate and $g : R^n \to R$ is a cost function, $g \in C^2$. Assume that all $\underline{\mathrm{f}}$ and $\overline{\mathrm{f}} \in D \subset R^n$ for some compact D. Then, to train the parameters $M^i_q \in \left[M^i_{q_1}, M^i_{q_2}\right]$ and σ^i_q, to minimize the squared errors given by (42), and to test for convergence, it is necessary to apply *Lemma 1* [69] to each of the lower and upper firing interval functions (23). Both are piecewise differentiable, i.e., each branch is differentiable [60] over its segment domain, and using the Taylor series expansion, it is possible to prove the next points:

1) $g(\underline{f}\,(new)) < g(\underline{f}\,(now))$ *if* $\nabla g(\underline{f}\,(now)) \neq 0$

$$g(\overline{f}\,(new)) < g(\overline{f}\,(now)) \text{ if } \nabla g(\overline{f}\,(now)) \neq 0$$

2) $\underline{f}(new) \to \underline{f}^*$ *as* $t \to \infty$

$$\overline{f}(new) \to \overline{f}^* \text{ as } t \to \infty$$

If $g(*)$ is bounded from below.

3) $\underline{f}^*$ is a local minimum of $g(\underline{f})$

$\overline{\overline{f}}^*$ is a local minimum of $g(\overline{\overline{f}})$

As for the convergence tuning of the centroid parameters $\left[\underline{c}^i_{l\alpha_k}, \overline{c}^i_{r\alpha_k}\right]$ the same Lemma 1 applies.

VI. SIMULATIONS

This section presents the experimental testing of the proposal, the prediction of the transfer bar surface temperature in an industrial hot strip mill facility located in Monterrey, México.

A. INPUT-OUTPUT DATA PAIRS

From an industrial HSM process, one hundred and seventy-five noisy input-output data pairs of three different types of coils, Table 9, were obtained and used as offline training data, (x'_1, x'_2, y). The inputs were x'_1, the transfer bar surface temperature measured by the pyrometer is located at the RM exit zone, and x'_2, the real time to move from the RM exit zone to the SB entry zone. The output y was the transfer bar surface temperature measured by the pyrometers located at the SB entry zone.

B. ANTECEDENT MEMBERSHIP FUNCTIONS

The primary membership functions for each antecedent of the base IT2α_0 NSFLS-2 were Gaussian functions with uncertain means $M^i_{q1\alpha_0}$, $M^i_{q2\alpha_0}$, and with the standard deviation $\sigma^i_{q\alpha_0}$, as shown in Tables 10 and 11. An array of two inputs, with five MF each, produces $M = 25$ rules.

C. FUZZY RULE BASE

The IT3 NSFLS-2 fuzzy rule base consists of a set of IF-THEN rules that represent the model of the complete system. The IT2α_0 NSFLS-2, that is the base of the 3D construction of the proposed fuzzy system, has two inputs x'_1 and x'_2 and one output y_α. The rule base has $M = 25$ rules of the type shown in Table 12.

D. FEEDBACK AND SIMULATION PROCESS

Three different sets of data for three different coil types were taken from a real mill. Each of these data sets was split into two sets: One for the initial adjustment and tuning process, and the other for the setup validation process. Eighty-three of type A, sixty-five of type B and twenty-seven of type C input-output data pairs were used for the initial offline training process, and seven input-output data pairs were used for testing. The production gage and width coil targets of the training data with the steel grade are shown in Table 9. In this initial offline process, computational time was not an issue. Table 13 shows the predicted temperature by the proposed

TABLE 5. Gradient descent equations for antecedent training under y_l contribution.

	Location of x'_q		Parameter of the antecedent membership function that contributes to the left-most section
1	$x'_q \leq M^i_{q1\alpha_0}$	$\overline{f}^i_{r\alpha_k} \in \left(\overline{f}^1_{r\alpha_k} \dots \overline{f}^L_{r\alpha_k}\right)$	$M^i_{q1\alpha_0}(new) = M^i_{q1\alpha_0}(now) + \frac{1}{2} K_{M_{q1\alpha_0}} e \sum_{k=1}^{2N} K_{\alpha_k} \left[\frac{\underline{c}^i_{l\alpha_k} - y_{l\alpha_k}}{\sum_{j=1}^{L} \overline{f}^j_{r\alpha_k} + \sum_{j=L+1}^{M} \underline{f}^j_{l\alpha_k}}\right] \left[\frac{1}{2} + \frac{\sqrt[2]{-2\,ln(\alpha_k)}}{z}\right] \left[\left(\frac{x'_q - M^i_{q1\alpha_0}}{\left(\sigma^i_{q\alpha_0}\right)^2 + \left(\sigma^i_{x_{q2}}\right)^2}\right) \overline{f}^i_{r\alpha_0}\right]$ $\sigma^i_{q\alpha_0}(new) = \sigma^i_{q\alpha_0}(now) + \frac{1}{2} K_{\sigma_q\alpha_0} e \sum_{k=1}^{2N} K_{\alpha_k} \left[\frac{\underline{c}^i_{l\alpha_k} - y_{l\alpha_k}}{\sum_{j=1}^{L} \overline{f}^j_{r\alpha_k} + \sum_{j=L+1}^{M} \underline{f}^j_{l\alpha_k}}\right] \left[\frac{1}{2} + \frac{\sqrt[2]{-2\,ln(\alpha_k)}}{z}\right] \left[\sigma^i_{q\alpha_0}\right] \left[\frac{\left(x'_q - M^i_{q1\alpha_0}\right)^2}{\left[\left(\sigma^i_{q\alpha_0}\right)^2 + \left(\sigma^i_{x_{q2}}\right)^2\right]^2} \overline{f}^i_{r\alpha_0}\right]$
2	$x'_q \geq M^i_{q2\alpha_0}$	$\overline{f}^i_{r\alpha_k} \in \left(\overline{f}^1_{r\alpha_k} \dots \overline{f}^L_{r\alpha_k}\right)$	$M^i_{q2\alpha_0}(new) = M^i_{q2\alpha_0}(now) + \frac{1}{2} K_{M_{q2\alpha_0}} e \sum_{k=1}^{2N} K_{\alpha_k} \left[\frac{\underline{c}^i_{l\alpha_k} - y_{l\alpha_k}}{\sum_{j=1}^{L} \overline{f}^i_{r\alpha_k} + \sum_{j=L+1}^{M} \underline{f}^i_{l\alpha_k}}\right] \left(\frac{1}{2} + \frac{\sqrt[2]{-2\,ln(\alpha_k)}}{z}\right) \left[\left(\frac{x'_q - M^i_{q2\alpha_0}}{\left(\sigma^i_{x_{q2}}\right)^2 + \left(\sigma^i_{q\alpha_0}\right)^2}\right) \overline{f}^i_{r\alpha_0}\right]$ $\sigma^i_{q\alpha_0}(new) = \sigma^i_{q\alpha_0}(now) + \frac{1}{2} K_{\sigma_q\alpha_0} e \sum_{k=1}^{2N} K_{\alpha_k} \left[\frac{\underline{c}^i_{l\alpha_k} - y_{l\alpha_k}}{\sum_{j=1}^{L} \overline{f}^i_{r\alpha_k} + \sum_{j=L+1}^{M} \underline{f}^i_{l\alpha_k}}\right] \left[\frac{1}{2} + \frac{\sqrt[2]{-2\,ln(\alpha_k)}}{z}\right] \left[\sigma^i_{q\alpha_0}\right] \left[\frac{\left(x'_q - M^i_{q2\alpha_0}\right)^2}{\left[\left(\sigma^i_{x_{q2}}\right)^2 + \left(\sigma^i_{q\alpha_0}\right)^2\right]^2} \overline{f}^i_{r\alpha_0}\right]$
3	$x'_q \leq \frac{M^i_{q1\alpha_0} + M^i_{q2\alpha_0}}{2} - \frac{\left(\sigma^i_{x_{q1}}\right)^2 \left(M^i_{q2\alpha_0} - M^i_{q1\alpha_0}\right)}{2\left(\sigma^i_{q\alpha_0}\right)^2}$	$\underline{f}^i_{l\alpha_k} \in \left(\underline{f}^{L+1}_{l\alpha_k} \dots \underline{f}^M_{l\alpha_k}\right)$	$M^i_{q2\alpha_0}(new) = M^i_{q2\alpha_0}(now) + \frac{1}{2} K_{M_{q2\alpha_0}} e \sum_{k=1}^{2N} K_{\alpha_k} \left[\frac{\underline{c}^i_{l\alpha_k} - y_{l\alpha_k}}{\sum_{j=1}^{L} \overline{f}^j_{r\alpha_k} + \sum_{j=L+1}^{M} \underline{f}^j_{l\alpha_k}}\right] \left(\frac{1}{2} + \frac{\sqrt[2]{-2\,ln(\alpha_k)}}{z}\right) \left[\left(\frac{x'_q - M^i_{q2\alpha_0}}{\left(\sigma^i_{x_{q1}}\right)^2 + \left(\sigma^i_{q\alpha_0}\right)^2}\right) \underline{f}^i_{l\alpha_0}\right]$ $\sigma^i_{q\alpha_0}(new) = \sigma^i_{q\alpha_0}(now) + \frac{1}{2} K_{\sigma_q\alpha_0} e \sum_{k=1}^{2N} K_{\alpha_k} \left[\frac{\underline{c}^i_{l\alpha_k} - y_{l\alpha_k}}{\sum_{j=1}^{L} \overline{f}^j_{r\alpha_k} + \sum_{j=L+1}^{M} \underline{f}^j_{l\alpha_k}}\right] \left[\frac{1}{2} + \frac{\sqrt[2]{-2\,ln(\alpha_k)}}{z}\right] \left[\sigma^i_{q\alpha_0}\right] \left[\frac{\left(x'_q - M^i_{q2\alpha_0}\right)^2}{\left[\left(\sigma^i_{x_{q1}}\right)^2 + \left(\sigma^i_{q\alpha_0}\right)^2 +\right]^2} \underline{f}^i_{l\alpha_0}\right]$
4	$x'_q \geq \frac{M^i_{q1\alpha_0} + M^i_{q2\alpha_0}}{2} + \frac{\left(\sigma^i_{x_{q1}}\right)^2 \left(M^i_{q2\alpha_0} - M^i_{q1\alpha_0}\right)}{2\left(\sigma^i_{q\alpha_0}\right)^2}$	$\underline{f}^i_{l\alpha_k} \in \left(\underline{f}^{L+1}_{l\alpha_k} \dots \underline{f}^M_{l\alpha_k}\right)$	$M^i_{q1\alpha_0}(new) = M^i_{q1\alpha_0}(now) + \frac{1}{2} K_{M_{q1\alpha_0}} e \sum_{k=1}^{2N} K_{\alpha_k} \left[\frac{\underline{c}^i_{l\alpha_k} - y_{l\alpha_k}}{\sum_{j=1}^{L} \overline{f}^j_{r\alpha_k} + \sum_{l=L+1}^{M} \underline{f}^j_{l\alpha_k}}\right] \left[\frac{1}{2} + \frac{\sqrt[2]{-2\,ln(\alpha_k)}}{z}\right] \left[\left(\frac{x'_q - M^i_{q1}}{\left(\sigma^i_{x_{q1}}\right)^2 + \left(\sigma^i_{q\alpha_0}\right)^2}\right) \underline{f}^i_{l\alpha_0}\right]$ $\sigma^i_{q\alpha_0}(new) = \sigma^i_{q\alpha_0}(now) + \frac{1}{2} K_{\sigma_q\alpha_0} e \sum_{k=1}^{2N} K_{\alpha_k} \left[\frac{\underline{c}^i_{l\alpha_k} - y_{l\alpha_k}}{\sum_{j=1}^{L} \overline{f}^j_{r\alpha_k} + \sum_{j=L+1}^{M} \underline{f}^j_{l\alpha_k}}\right] \left[\frac{1}{2} + \frac{\sqrt[2]{-2\,\ln(\alpha_k)}}{z}\right] \left[\sigma^i_{q\alpha_0}\right] \left[\frac{\left(x'_q - M^i_{q1\alpha_0}\right)^2}{\left[\left(\sigma^i_{x_{q1}}\right)^2 + \left(\sigma^i_{q\alpha_0}\right)^2\right]^2} \underline{f}^i_{l\alpha_0}\right]$

TABLE 6. Gradient descent equations for antecedent training under y_r contribution.

	Location of x'_q		Parameter of the antecedent membership function that contributes to the right-most section
1	$x'_q \leq M^i_{q1\alpha_0}$	$\overline{f}^i_{r\alpha_k} \in \left(\overline{f}^{R+1}_{r\alpha_k} \dots \overline{f}^{M}_{r\alpha_k}\right)$	$\begin{aligned} M^i_{q1\alpha_0}(new) &= M^i_{q1\alpha_0}(now) + \frac{1}{2} K_{M_{q1\alpha_0}} e \sum_{k=1}^{2N} K_{\alpha_k} \left[\frac{\overline{c}^i_{r\alpha_k} - y_{r\alpha_k}}{\sum_{j=1}^{R} \underline{f}^j_{l\alpha_k} + \sum_{j=R+1}^{M} \overline{f}^j_{r\alpha_k}}\right]\left[\frac{1}{2} + \frac{\sqrt[2]{-2\ln(\alpha_k)}}{z}\right]\left[\left(\frac{x'_q - M^i_{q1\alpha_0}}{\left(\sigma^i_{x_{q2}}\right)^2 + \left(\sigma^i_{q\alpha_0}\right)^2}\right)\overline{f}^i_{r\alpha_0}\right] \\ \sigma^i_{q\alpha_0}(new) &= \sigma^i_{q\alpha_0}(now) + \frac{1}{2} K_{\sigma_{q\alpha_0}} e \sum_{k=1}^{2N} K_{\alpha_k} \left[\frac{\overline{c}^i_{r\alpha_k} - y_{r\alpha_k}}{\sum_{j=1}^{R} \underline{f}^i_{l\alpha_k} + \sum_{j=R+1}^{M} \overline{f}^j_{r\alpha_k}}\right]\left[\frac{1}{2} + \frac{\sqrt[2]{-2\ln(\alpha_k)}}{z}\right]\left[\sigma^i_{q\alpha_0}\right]\left[\frac{\left(x'_q - M^i_{q1\alpha_0}\right)^2}{\left[\left(\sigma^i_{x_{q2}}\right)^2 + \left(\sigma^i_{q\alpha_0}\right)^2\right]^2}\overline{f}^i_{r\alpha_0}\right] \end{aligned}$
2	$x'_q \geq M^i_{q2\alpha_0}$	$\overline{f}^i_{r\alpha_k} \in \left(\overline{f}^{R+1}_{r\alpha_k} \dots \overline{f}^{M}_{r\alpha_k}\right)$	$\begin{aligned} M^i_{q2\alpha_0}(new) &= M^i_{q2\alpha_0}(now) + \frac{1}{2} K_{M_{q2\alpha_0}} e \sum_{k=1}^{2N} K_{\alpha_k} \left[\frac{\overline{c}^i_{r\alpha_k} - y_{r\alpha_k}}{\sum_{j=1}^{R} \underline{f}^j_{l\alpha_k} + \sum_{j=R+1}^{M} \overline{f}^j_{r\alpha_k}}\right]\left(\frac{1}{2} + \frac{\sqrt[2]{-2\ln(\alpha_k)}}{z}\right)\left[\left(\frac{x'_q - M^i_{q2\alpha_0}}{\left(\sigma^i_{x_{q2}}\right)^2 + \left(\sigma^i_{q\alpha_0}\right)^2}\right)\overline{f}^i_{r\alpha_0}\right] \\ \sigma^i_{q\alpha_0}(new) &= \sigma^i_{q\alpha_0}(now) + \frac{1}{2} K_{\sigma_{q\alpha_0}} e \sum_{k=1}^{2N} K_{\alpha_k} \left[\frac{\overline{c}^i_{r\alpha_k} - y_{r\alpha_k}}{\sum_{j=1}^{R} \underline{f}^j_{l\alpha_k} + \sum_{j=R+1}^{M} \overline{f}^j_{r\alpha_k}}\right]\left[\frac{1}{2} + \frac{\sqrt[2]{-2\ln(\alpha_k)}}{z}\right]\left[\sigma^i_{q\alpha_0}\right]\left[\frac{\left(x'_q - M^i_{q2\alpha_0}\right)^2}{\left[\left(\sigma^i_{x_{q2}}\right)^2 + \left(\sigma^i_{q\alpha_0}\right)^2\right]^2}\overline{f}^i_{r\alpha_0}\right] \end{aligned}$
3	$x'_q \leq \frac{M^i_{q1\alpha_0} + M^i_{q2\alpha_0}}{2} - \frac{\left(\sigma^i_{x_{q1}}\right)^2\left(M^i_{q2\alpha_0} - M^i_{q1\alpha_0}\right)}{2\left(\sigma^i_{q\alpha_0}\right)^2}$	$\underline{f}^i_{l\alpha_k} \in \left(\underline{f}^1_{l\alpha_k} \dots \underline{f}^R_{l\alpha_k}\right)$	$\begin{aligned} M^i_{q2\alpha_0}(new) &= M^i_{q2\alpha_0}(now) + \frac{1}{2} K_{M_{q2\alpha_0}} e \sum_{k=1}^{2N} K_{\alpha_k} \left[\frac{\overline{c}^i_{r\alpha_k} - y_{r\alpha_k}}{\sum_{j=1}^{R} \underline{f}^i_{l\alpha_k} + \sum_{j=R+1}^{M} \overline{f}^i_{r\alpha_k}}\right]\left(\frac{1}{2} + \frac{\sqrt[2]{-2\ln(\alpha_k)}}{z}\right)\left[\left(\frac{x'_q - M^i_{q2\alpha_0}}{\left(\sigma^i_{x_{q1}}\right)^2 + \left(\sigma^i_{q}\right)^2}\right)\underline{f}^i_{l\alpha_0}\right] \\ \sigma^i_{q\alpha_0}(new) &= \sigma^i_{q\alpha_0}(now) + \frac{1}{2} K_{\sigma_{q\alpha_0}} e \sum_{k=1}^{2N} K_{\alpha_k} \left[\frac{\overline{c}^i_{r\alpha_k} - y_{r\alpha_k}}{\sum_{j=1}^{R} \underline{f}^j_{l\alpha_k} + \sum_{j=R+1}^{M} \overline{f}^j_{r\alpha_k}}\right]\left[\frac{1}{2} + \frac{\sqrt[2]{-2\ln(\alpha_k)}}{z}\right]\left[\sigma^i_{q\alpha_0}\right]\left[\frac{\left(x'_q - M^i_{q2\alpha_0}\right)^2}{\left[\left(\sigma^i_{x_{q1}}\right)^2 + \left(\sigma^i_{q\alpha_0}\right)^2\right]^2}\underline{f}^i_{l\alpha_0}\right] \end{aligned}$
4	$x'_q \geq \frac{M^i_{q1\alpha_0} + M^i_{q2\alpha_0}}{2} + \frac{\left(\sigma^i_{x_{q1}}\right)^2\left(M^i_{q2\alpha_0} - M^i_{q1\alpha_0}\right)}{2\left(\sigma^i_{q\alpha_0}\right)^2}$	$\underline{f}^i_{l\alpha_k} \in \left(\underline{f}^1_{l\alpha_k} \dots \underline{f}^R_{l\alpha_k}\right)$	$\begin{aligned} M^i_{q1\alpha_0}(new) &= M^i_{q1\alpha_0}(now) + \frac{1}{2} K_{M_{q1\alpha_0}} e \sum_{k=1}^{2N} K_{\alpha_k} \left[\frac{\overline{c}^i_{r\alpha_k} - y_{r\alpha_k}}{\sum_{j=1}^{R} \underline{f}^j_{l\alpha_k} + \sum_{j=R+1}^{M} \overline{f}^j_{r\alpha_k}}\right]\left[\frac{1}{2} + \frac{\sqrt[2]{-2\ln(\alpha_k)}}{z}\right]\left[\left(\frac{x'_q - M^i_{q1\alpha_0}}{\left(\sigma^i_{x_{q1}}\right)^2 + \left(\sigma^i_{q\alpha_0}\right)^2}\right)\underline{f}^i_{l\alpha_0}\right] \\ \sigma^i_{q\alpha_0}(new) &= \sigma^i_{q\alpha_0}(now) + \frac{1}{2} K_{\sigma_{q\alpha_0}} e \sum_{k=1}^{2N} K_{\alpha_k} \left[\frac{\overline{c}^i_{r\alpha_k} - y_{r\alpha_k}}{\sum_{j=1}^{R} \underline{f}^j_{l\alpha_k} + \sum_{j=R+1}^{M} \overline{f}^j_{r\alpha_k}}\right]\left[\frac{1}{2} + \frac{\sqrt[2]{-2\ln(\alpha_k)}}{z}\right]\left[\sigma^i_{q\alpha_0}\right]\left[\frac{\left(x'_q - M^i_{q1\alpha_0}\right)^2}{\left[\left(\sigma^i_{x_{q1}}\right)^2 + \left(\sigma^i_{q\alpha_0}\right)^2\right]^2}\underline{f}^i_{l\alpha_0}\right] \end{aligned}$

TABLE 7. Gradient descent equations for $\underline{c}^i_{l\alpha_0}$ consequent training.

	Contribution to the left-most section
$\overline{f}^i_{r\alpha_k} \in \left(\overline{f}^1_{r\alpha_k} \dots \overline{f}^L_{r\alpha_k}\right)$	$\underline{c}^i_{l\alpha_0}(new) = \underline{c}^i_{l\alpha_0}(now) + \frac{1}{2} K_{\underline{c}_l\alpha_0} e \sum_{k=1}^{2N} K_{\alpha_k} \left[\frac{\overline{f}^i_{r\alpha_k}}{\sum_{j=1}^{L}\overline{f}^j_{r\alpha_k} + \sum_{j=L+1}^{M}\underline{f}^j_{l\alpha_k}}\right]\left[\frac{1}{2} + \frac{\sqrt[2]{-2\,ln(\alpha_k)}}{z}\right]$
$\underline{f}^i_{l\alpha_k} \in \left(\underline{f}^{L+1}_{l\alpha_k} \dots \underline{f}^M_{l\alpha_k}\right)$	$\underline{c}^i_{l\alpha_0}(new) = \underline{c}^i_{l\alpha_0}(now) + \frac{1}{2} K_{\underline{c}_l\alpha_0} e \sum_{k=1}^{2N} K_{\alpha_k} \left[\frac{\underline{f}^i_{l\alpha_k}}{\sum_{j=1}^{L}\overline{f}^j_{r\alpha_k} + \sum_{j=L+1}^{M}\underline{f}^j_{l\alpha_k}}\right]\left[\frac{1}{2} + \frac{\sqrt[2]{-2\,ln(\alpha_k)}}{z}\right]$

TABLE 8. Gradient descent equations for $\overline{c}^i_{r\alpha_0}$ consequent training.

	Contribution to the right-most section
$\underline{f}^i_{l\alpha_k} \in \left(\underline{f}^1_{l\alpha_k} \dots \underline{f}^R_{l\alpha_k}\right)$	$\overline{c}^i_{r\alpha_0}(new) = \overline{c}^i_{r\alpha_0}(now) + \frac{1}{2} K_{\overline{c}_r\alpha_0} e \sum_{k=1}^{2N} K_{\alpha_k} \left[\frac{\underline{f}^i_{l\alpha_k}}{\sum_{j=1}^{R}\underline{f}^j_{l\alpha_k} + \sum_{j=R+1}^{M}\overline{f}^j_{r\alpha_k}}\right]\left[\frac{1}{2} + \frac{\sqrt[2]{-2\,ln(\alpha_k)}}{z}\right]$
$\overline{f}^i_{r\alpha_k} \in \left(\overline{f}^{R+1}_{r\alpha_k} \dots \overline{f}^M_{r\alpha_k}\right)$	$\overline{c}^i_{r\alpha_0}(new) = \overline{c}^i_{r\alpha_0}(now) + \frac{1}{2} K_{\overline{c}_r\alpha_0} e \sum_{k=1}^{2N} K_{\alpha_k} \left[\frac{\overline{f}^i_{r\alpha_k}}{\sum_{j=1}^{R}\overline{f}^j_{r\alpha_k} + \sum_{j=R+1}^{M}\underline{f}^j_{l\alpha_k}}\right]\left[\frac{1}{2} + \frac{\sqrt[2]{-2\,ln(\alpha_k)}}{z}\right]$

TABLE 9. Type of coils.

Coil type	Target gage (mm)	Target width (mm)	Steel grade (SAE-AISI)
A	1.879	1041.0	1006
B	2.006	991.0	1006
C	2.159	952.0	1006

TABLE 10. Parameters for MF of x'_1 input.

	$M^i_{11\alpha_0}$ (°C)	$M^i_{12\alpha_0}$ (°C)	$\sigma^i_{1\alpha_0}$ (°C)
1	1010	1012	30
2	1040	1042	30
3	1070	1072	30
4	1100	1102	30
5	1130	1132	30

TABLE 11. Parameters for MF of x'_2 input.

	$M^i_{21\alpha_0}$ (s)	$M^i_{22\alpha_0}$ (s)	$\sigma^i_{2\alpha_0}$ (s)
1	32.16	32.66	2.72
2	34.88	35.38	2.72
3	37.60	38.10	2.72
4	40.32	40.82	2.72
5	43.04	43.54	2.72

TABLE 12. Fuzzy rule base.

Rule	$M^i_{12\alpha_0}$ (°C)	$M^i_{12\alpha_0}$ (°C)	$\sigma^i_{1\alpha_0}$ (°C)	$M^i_{21\alpha_0}$ (s)	$M^i_{22\alpha_0}$ (s)	$\sigma^i_{2\alpha_0}$ (s)	$\underline{c}^i_{l\alpha_0}$ (°C)	$\overline{\sigma}^i_{r\alpha_0}$ (°C)
1	1010	1012	30	32.16	32.66	2.7	960	962
2	1010	1012	30	34.88	35.38	2.7	958	960
3	1010	1012	30	37.60	38.10	2.7	956	958
4	1010	1012	30	40.32	40.82	2.7	954	956
5	1010	1012	30	43.04	43.54	2.7	952	954
6	1040	1042	30	32.16	32.66	2.7	970	972
7	1040	1042	30	34.88	35.38	2.7	968	970
8	1040	1042	30	37.60	38.10	2.7	966	968
9	1040	1042	30	40.32	40.82	2.7	964	966
10	1040	1042	30	43.04	43.54	2.7	962	964
11	1070	1072	30	32.16	32.66	2.7	980	982
12	1070	1072	30	34.88	35.38	2.7	978	980
13	1070	1072	30	37.60	38.10	2.7	976	978
14	1070	1072	30	40.32	40.82	2.7	974	976
15	1070	1072	30	43.04	43.54	2.7	972	974
16	1100	1102	30	32.16	32.66	2.7	990	992
17	1100	1102	30	34.88	35.38	2.7	988	990
18	1100	1102	30	37.60	38.10	2.7	986	988
19	1100	1102	30	40.32	40.82	2.7	984	986
20	1100	1102	30	43.04	43.54	2.7	982	984
21	1130	1132	30	32.16	32.66	2.7	1000	1002
22	1130	1132	30	34.88	35.38	2.7	998	1000
23	1130	1132	30	37.60	38.10	2.7	996	998
24	1130	1132	30	40.32	40.82	2.7	994	996
25	1130	1132	30	43.04	43.54	2.7	992	994

IT3 NSFLS-2 and as compared to type-1 (T1), IT2 NSFLS-2 and GT2 NSFLS-2 fuzzy systems. A Dell PC i7, 16 GB RAM memory and 2.8 GHz using Win 11 HSL OS was used to execute the fuzzy systems programed in MS VS 2022 C++ Language.

TABLE 13. Estimated vs. objective transfer bar surface temperature (°C).

No. of data pair	1	2	3	4	5	6	7
Objective	994.5	984.4	993.1	991.7	986.7	981.6	976.6
T1 SFLS	979.8	977.1	979.2	978.3	976.9	974.7	972.4
T1 RBFNN	978.4	977.0	978.1	977.6	976.9	975.9	974.7
IT2	992.2	987.4	991.5	990.8	986.7	981.6	976.3
GT2 1 level-$\boldsymbol{\alpha}_k$	992.2	987.2	991.4	990.7	986.7	981.6	976.8
GT2 10 levels-$\boldsymbol{\alpha}_k$	992.6	987.3	991.8	990.8	986.7	981.6	976.5
GT2 100 levels-$\boldsymbol{\alpha}_k$	992.6	987.3	993.1	990.9	986.6	981.5	976.5
GT2 1000 levels-$\boldsymbol{\alpha}_k$	992.3	987.2	993.1	990.8	986.5	981.5	976.6
IT3 1 level-$\boldsymbol{\alpha}_k$	993.2	987.2	991.4	990.7	986.7	981.6	976.8
IT3 10 levels-$\boldsymbol{\alpha}_k$	993.7	987.3	991.8	990.8	986.7	981.6	976.5
IT3 100 levels-$\boldsymbol{\alpha}_k$	993.8	987.3	993.1	990.9	986.6	981.5	976.5
IT3 1000 levels-$\boldsymbol{\alpha}_k$	993.7	987.2	993.1	990.8	986.5	981.5	976.6

TABLE 14. RMSE (°C) of 7 input-output data pairs for temperature estimation and for antecedent and consequent parameters update. 20 epochs of training.

	0 levels-α_k	1 level-α_k	10 levels-α_k	100 levels-α_k	1000 levels-α_k
T1 SFLS	3.1667				
T1 RBFNN	3.1622				
IT2 NSFLS-2	1.0757	-	-	-	-
GT2 NSFLS-2	-	1.0690	1.0071	0.9180	0.9411
IT3 NSFLS-2	-	1	0.9258	0.8194	0.8280

TABLE 15. Computational time (s) used to update the antecedent and consequent parameters.

	0 levels-α_k	1 level-α_k	10 levels-α_k	100 levels-α_k	1000 levels-α_k
IT2 NSFLS-2	0.458	-	-	-	-
GT2 NSFLS-2	-	0.489	0.722	0.981	1.212
IT3 NSFLS-2	-	0.568	0.798	0.995	1.315

Seven input-output data pairs were used to test the offline SB entry temperature estimation. The prediction results obtained with T1 systems, and IT2 benchmark models are shown in Fig. 8, while the prediction of the GT2 and the proposed IT3 systems using different levels-α are shown in Fig. 9. Table 14, Fig. 10, and Fig. 11 show the root mean square error (RMSE) behavior of the GT2 systems vs. the performance of the proposed IT3 systems using 1, 10, 100 and 1000 levels-α. Fig. 10 shows the performance using only 1 level-α, while Fig. 11 shows the performance using 1, 10, 100 and 1000 levels-α. The time used to calculate the temperature and to update its parameters is shown in Tabl. 15 and Fig. 12.

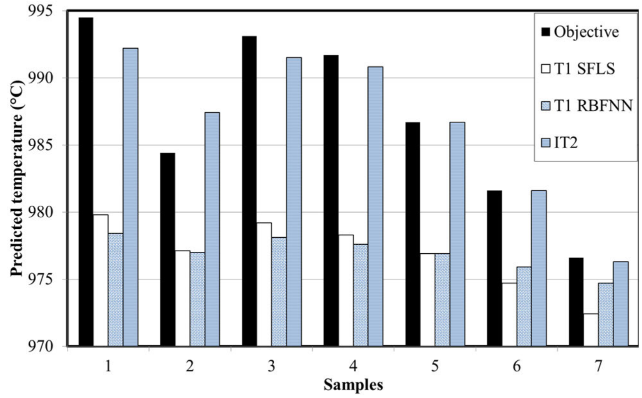

FIGURE 8. Benchmark results of prediction of T1 and IT2 models.

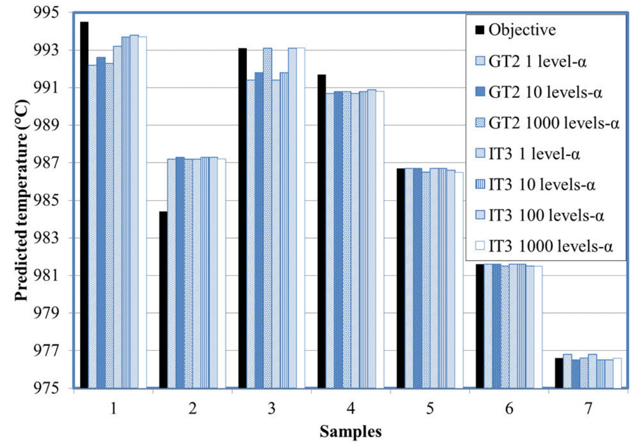

FIGURE 9. Benchmark results of prediction of GT2 NSFLS-2 and IT3 NSFLS-2.

Twenty epochs of training were chosen for offline tuning. The exclusive usage of validated and bounded input-output data pairs guarantees the convergence of the proposed IT3 NSFLS-2, as proved experimentally in this research. The proposed training method gave the IT3 NSFLS-2 presented the better performance, but computational time was higher than that of the IT2 NSFLS-2 and the GT2 NSFLS-2, as shown in Fig. 12.

The results show that the best estimation is obtained by the IT3 NSFLS-2 model using 100 levels-α with a RMSE $=$ 0.8194°. Both the IT3 NSFLS-2 using 10 and 1000 levels- α presented the values of RMSE=0.9258°C and RMSE=0.8280°C, respectively. An unexpected result is shown with the RMSE produced using 100 levels-α: It is better than that produced by the IT2 NSFLS-2, GT2 NSFLS-2, and the result obtained by the T1 radial basis function neural network (T1 RBFNN) and by the type-1 singleton fuzzy logic system (T1 SFLS).

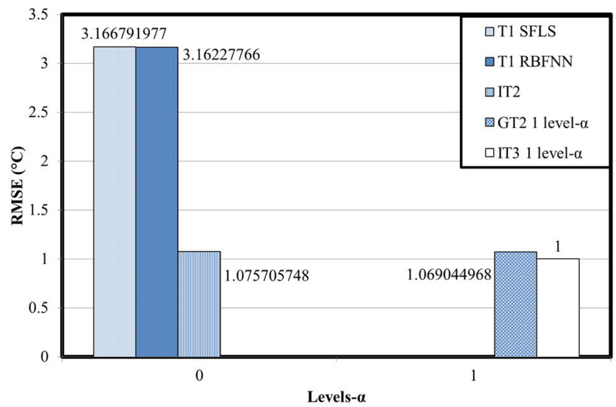

FIGURE 10. IT3 NSFLS-2 RMSE (°C) compared with T1, IT2 NSFLS-2, and GT2 NSFLS-2 models.

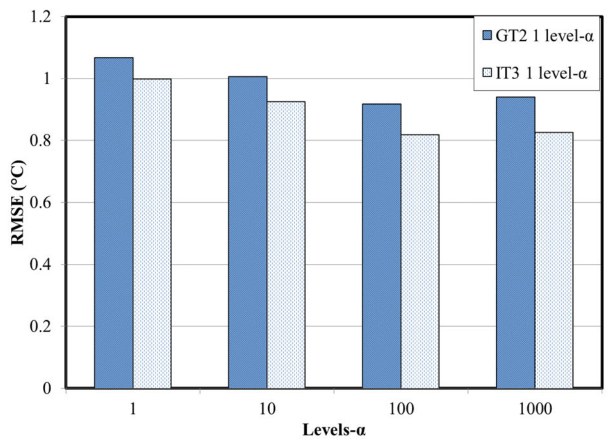

FIGURE 11. IT3 NSFLS-2 RMSE (°C) compared with GT2 NSFLS-2 models with different levels-α.

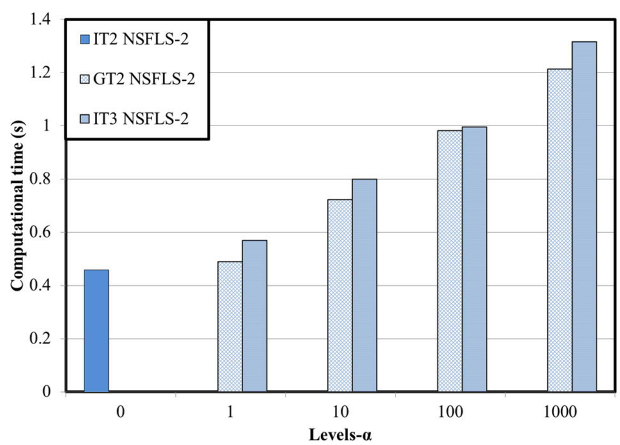

FIGURE 12. Computational time (s) of IT2 NSFLS-2, GT2 NSFL-2 and IT3 NSFLS-2 models.

VII. CONCLUSION

Based on mathematical foundations for classical fuzzy systems, this paper presents a new method to construct and train IT3 NSFLS-2 systems whose inputs are modeled as type-2 non-singleton numbers. A real-world problem of predicting the surface temperature of a transfer bar in a hot strip mill as a case study was introduced and compared with similar methods.

Benchmark results showed that our method presented superior performance capabilities when compared to conventional IT2, GT2 and IT3 NSFLS-2 systems. It was shown that our method used few training epochs, showed stable convergence and lower RMSE values. Best results for the proposed system occurred when using 100 levels-α. The lower error was obtained when using the first level-α_0 to estimate the firing intervals and the centroids instead of the traditional calculation process used in conventional models.

Experimental results also showed that computational times for the IT2 NSFLS-2, GT2 NSFLS-2, and the proposed IT3 NSFLS-2 were less than 1 second, which is considered appropriate for controlling industrial processes.

The knowledge gap of using type-2 non-singleton numbers to model the system's inputs, and the use of Gaussians with variable mean and fixed standard deviation to model the MFs of antecedents and consequent has been covered with our method. As future work, we have envisaged the application of our method to other industrial cases as well as further mathematical analysis in control theory regarding its robustness and stability proof using Lyapunov theory.

REFERENCES

[1] J. T. Rickard, J. Aisbett, and G. Gibbon, "Fuzzy subsethood for fuzzy sets of type-2 and generalized type-*n*," *IEEE Trans. Fuzzy Syst.*, vol. 17, no. 1, pp. 50–60, Feb. 2008, doi: 10.1109/TFUZZ.2008.2006369.

[2] J. T. Rickard, J. Aisbett, G. Gibbon, and D. Morgenthaler, "Fuzzy subsethood for type-n fuzzy sets," in *Proc. Annu. Meeting North Amer. Fuzzy Inf. Process. Soc.*, 2008, pp. 1–6, doi: 10.1109/NAFIPS.2008.4531276.

[3] A. Chaudhuri, "Forecasting rice production in West Bengal state in India: Statistical vs. computational intelligence techniques," *Int. J. Agricult. Environ. Inf. Syst.*, vol. 4, no. 4, pp. 68–91, Oct. 2013, doi: 10.4018/ijaeis.2013100104.

[4] O. Castillo, J. R. Castro, and P. Melin, *Interval Type-3 Fuzzy Systems: Theory and Design*, 1st ed. Cham, Switzerland: Springer, 2022, pp. 1–100, doi: 10.1007/978-3-030-96515-0.

[5] O. Castillo, J. R. Castro, and P. Melin, "Interval type-3 fuzzy fractal approach in sound speaker quality control evaluation," *Eng. Appl. Artif. Intell.*, vol. 116, Nov. 2022, Art. no. 105363, doi: 10.1016/j.engappai.2022.105363.

[6] O. Castillo and P. Melin, "Towards interval type-3 intuitionistic fuzzy sets and systems," *Mathematics*, vol. 10, no. 21, p. 4091, Nov. 2022, doi: 10.3390/math10214091.

[7] C. Peraza, P. Ochoa, O. Castillo, and Z. W. Geem, "Interval-type 3 fuzzy differential evolution for designing an interval-type 3 fuzzy controller of a unicycle mobile robot," *Mathematics*, vol. 10, no. 19, p. 3533, Sep. 2022, doi: 10.3390/math10193533.

[8] L. Amador-Angulo, O. Castillo, P. Melin, and J. R. Castro, "Interval type-3 fuzzy adaptation of the bee colony optimization algorithm for optimal fuzzy control of an autonomous mobile robot," *Micromachines*, vol. 13, no. 9, p. 1490, Sep. 2022, doi: 10.3390/mi13091490.

[9] O. Castillo, J. R. Castro, and P. Melin, "Interval type-3 fuzzy control for automated tuning of image quality in televisions," *Axioms*, vol. 11, no. 6, p. 276, Jun. 2022, doi: 10.3390/axioms11060276.

[10] O. Castillo, J. R. Castro, and P. Melin, "Forecasting the COVID-19 with interval type-3 fuzzy logic and the fractal dimension," *Int. J. Fuzzy Syst.*, vol. 37, no. 10, pp. 7909–7943, 2022, doi: 10.1007/s40815-022-01351-7.

[11] O. Castillo, J. R. Castro, and P. Melin, "A methodology for building interval type-3 fuzzy systems based on the principle of justifiable granularity," *Int. J. Intell. Syst.*, vol. 37, no. 10, pp. 7909–7943, Oct. 2022, doi: 10.1002/int.22910.

[12] O. Castillo, M. Pulido, and P. Melin, "Interval type-3 fuzzy aggregators for ensembles of neural networks in time series prediction," in *Proc. Int. Conf. Intell. Fuzzy Syst.* Cham, Switzerland: Springer, 2022, pp. 785–793.

[13] O. Castillo, J. R. Castro, and P. Melin, "Interval type-3 fuzzy aggregation of neural networks for multiple time series prediction: The case of financial forecasting," *Axioms*, vol. 11, no. 6, p. 251, May 2022.

[14] O. Castillo, J. R. Castro, M. Pulido, and P. Melin, "Interval type-3 fuzzy aggregators for ensembles of neural networks in COVID-19 time series prediction," *Eng. Appl. Artif. Intel.*, vol. 114, pp. 105–110, 2022, doi: 10.1016/j.engappai.2022.105110.

[15] A. Mohammadzadeh, O. Castillo, S. S. Band, and A. Mosavi, "A novel fractional-order multiple-model type-3 fuzzy control for nonlinear systems with unmodeled dynamics," *Int. J. Fuzzy Syst.*, vol. 23, no. 6, pp. 1633–1651, Sep. 2021, doi: 10.1007/s40815-021-01058-1.

[16] A. A. Aly, B. F. Felemban, A. Mohammadzadeh, O. Castillo, and A. Bartoszewicz, "Frequency regulation system: A deep learning identification, type-3 fuzzy control and LMI stability analysis," *Energies*, vol. 14, no. 22, p. 7801, Nov. 2021, doi: 10.3390/en14227801.

[17] O. Castillo, F. Valdez, C. Peraza, J. H. Yoon, and Z. W. Geem, "High-speed interval type-2 fuzzy systems for dynamic parameter adaptation in harmony search for optimal design of fuzzy controllers," *Mathematics*, vol. 9, no. 7, p. 758, Apr. 2021, doi: 10.3390/math9070758.

[18] P. Melin, D. Sánchez, J. R. Castro, and O. Castillo, "Design of type-3 fuzzy systems and ensemble neural networks for COVID-19 time series prediction using a firefly algorithm," *Axioms*, vol. 11, no. 8, p. 410, Aug. 2022, doi: 10.3390/axioms11080410.

[19] V. Kreinovich, O. Kosheleva, P. Melin, and O. Castillo, "Efficient algorithms for data processing under type-3 (and higher) fuzzy uncertainty," *Mathematics*, vol. 10, no. 13, p. 2361, Jul. 2022, doi: 10.3390/math10132361.

[20] Z. Liu, A. Mohammadzadeh, H. Turabieh, M. Mafarja, S. S. Band, and A. Mosavi, "A new online learned interval type-3 fuzzy control system for solar energy management systems," *IEEE Access*, vol. 9, pp. 10498–10508, 2021, doi: 10.1109/ACCESS.2021.3049301.

[21] A. Mohammadzadeh, M. H. Sabzalian, and W. Zhang, "An interval type-3 fuzzy system and a new online fractional-order learning algorithm: Theory and practice," *IEEE Trans. Fuzzy Syst.*, vol. 28, no. 9, pp. 1940–1950, Sep. 2020, doi: 10.1109/TFUZZ.2019.2928509.

[22] M.-W. Tian, S.-R. Yan, A. Mohammadzadeh, J. Tavoosi, S. Mobayen, R. Safdar, W. Assawinchaichote, M. T. Vu, and A. Zhilenkov, "Stability of interval type-3 fuzzy controllers for autonomous vehicles," *Mathematics*, vol. 9, no. 21, p. 2742, Oct. 2021, doi: 10.3390/math9212742.

[23] A. Taghieh, A. Mohammadzadeh, C. Zhang, S. Rathinasamy, and S. Bekiros, "A novel adaptive interval type-3 neuro-fuzzy robust controller for nonlinear complex dynamical systems with inherent uncertainties," *Nonlinear Dyn.*, vol. 2022, pp. 1–15, Jan. 2022, doi: 10.1007/s11071-022-07867-9.

[24] D. Singh, N. Verma, A. Ghosh, and A. Malagaudanavar, "An approach towards the design of interval type-3 T–S fuzzy system," *IEEE Trans. Fuzzy Syst.*, vol. 30, no. 9, pp. 3880–3893, Sep. 2022, doi: 10.1109/TFUZZ.2021.3133083.

[25] M. Gheisarnejad, A. Mohammadzadeh, and M.-H. Khooban, "Model predictive control based type-3 fuzzy estimator for voltage stabilization of DC power converters," *IEEE Trans. Ind. Electron.*, vol. 69, no. 12, pp. 13849–13858, Dec. 2022, doi: 10.1109/TIE.2021.3134052.

[26] S. N. Qasem, A. Ahmadian, A. Mohammadzadeh, S. Rathinasamy, and B. Pahlevanzadeh, "A type-3 logic fuzzy system: Optimized by a correntropy based Kalman filter with adaptive fuzzy kernel size," *Inf. Sci.*, vol. 572, pp. 424–443, Sep. 2021, doi: 10.1016/j.ins.2021.05.031.

[27] M. Gheisarnejad, A. Mohammadzadeh, H. Farsizadeh, and M.-H. Khooban, "Stabilization of 5G telecom converter-based deep type-3 fuzzy machine learning control for telecom applications," *IEEE Trans. Circuits Syst. II, Exp. Briefs*, vol. 69, no. 2, pp. 544–548, Feb. 2022, doi: 10.1109/TCSII.2021.3102282.

[28] A. Taghieh, A. Mohammadzadeh, C. Zhang, N. Kausar, and O. Castillo, "A type-3 fuzzy control for current sharing and voltage balancing in microgrids," *Appl. Soft Comput.*, vol. 129, Nov. 2022, Art. no. 109636, doi: 10.1016/j.asoc.2022.109636.

[29] A. Taghieh, C. Zhang, K. A. Alattas, Y. Bouteraa, S. Rathinasamy, and A. Mohammadzadeh, "A predictive type-3 fuzzy control for underactuated surface vehicles," *Ocean Eng.*, vol. 266, Dec. 2022, Art. no. 113014, doi: 10.1016/j.oceaneng.2022.113014.

[30] J.-H. Wang, J. Tavoosi, A. Mohammadzadeh, S. Mobayen, J. H. Asad, W. Assawinchaichote, M. T. Vu, and P. Skruch, "Non-singleton type-3 fuzzy approach for flowmeter fault detection: Experimental study in a gas industry," *Sensors*, vol. 21, no. 21, p. 7419, Nov. 2021, doi: 10.3390/s21217419.

[31] M. A. Balootaki, H. Rahmani, H. Moeinkhah, and A. Mohammadzadeh, "Non-singleton fuzzy control for multi-synchronization of chaotic systems," *Appl. Soft Comput.*, vol. 99, Feb. 2021, Art. no. 106924, doi: 10.1016/j.asoc.2020.106924.

[32] K. A. Alattas, A. Mohammadzadeh, S. Mobayen, A. A. Aly, B. F. Felemban, and M. T. Vu, "A new data-driven control system for MEMSs gyroscopes: Dynamics estimation by type-3 fuzzy systems," *Micromachines*, vol. 12, no. 11, p. 1390, Nov. 2021, doi: 10.3390/mi12111390.

[33] M. S. S. S. Amirhosein Mosavi, S. N. Qasem, and A. Mohammadzadeh, "Fractional-order fuzzy control approach for photovoltaic/battery systems under unknown dynamics, variable irradiation and temperature," *Electronics*, vol. 9, p. 1455, Sep. 2020, doi: 10.3390/electronics9091455.

[34] M.-W. Tian, A. Mohammadzadeh, J. Tavoosi, S. Mobayen, J. H. Asad, O. Castillo, and A. R. Várkonyi-Kóczy, "A deep-learned type-3 fuzzy system and its application in modeling problems," *Acta Polytechnica Hungarica*, vol. 19, no. 2, pp. 151–172, 2022, doi: 10.12700/aph.19.2.2022.2.9.

[35] M.-W. Tian, Y. Bouteraa, K. A. Alattas, S.-R. Yan, A. K. Alanazi, A. Mohammadzadeh, and S. Mobayen, "A type-3 fuzzy approach for stabilization and synchronization of chaotic systems: Applicable for financial and physical chaotic systems," *Complexity*, vol. 2022, pp. 1–17, Jun. 2022, doi: 10.1155/2022/8437910.

[36] A. Mohammadzadeh and R. H. Vafaie, "A deep learned fuzzy control for inertial sensing: Micro electro mechanical systems," *Appl. Soft Comput.*, vol. 109, Sep. 2021, Art. no. 107597, doi: 10.1016/j.asoc.2021.107597.

[37] N. Nabipour, S. N. Qasem, and K. Jermsittiparsert, "Type-3 fuzzy voltage management in PV/hydrogen fuel cell/battery hybrid systems," *Int. J. Hydrogen Energy*, vol. 45, no. 56, pp. 32478–32492, 2020, doi: 10.1016/j.ijhydene.2020.08.261.

[38] G. Hua, F. Wang, J. Zhang, K. A. Alattas, A. Mohammadzadeh, and M. T. Vu, "A new type-3 fuzzy predictive approach for mobile robots," *Mathematics*, vol. 10, no. 17, p. 3186, Sep. 2022, doi: 10.3390/math10173186.

[39] S. Yan, A. A. Aly, B. F. Felemban, M. Gheisarnejad, M. Tian, M. H. Khooban, A. Mohammadzadeh, and S. Mobayen, "A new event-triggered type-3 fuzzy control system for multi-agent systems: Optimal economic efficient approach for actuator activating," *Electronics*, vol. 10, no. 24, p. 3122, Dec. 2021, doi: 10.3390/electronics10243122.

[40] Y. Cao, A. Raise, A. Mohammadzadeh, S. Rathinasamy, S. S. Band, and A. Mosavi, "Deep learned recurrent type-3 fuzzy system: Application for renewable energy modeling/prediction," *Energy Rep.*, vol. 7, pp. 8115–8127, Nov. 2021, doi: 10.1016/j.egyr.2021.07.004.

[41] C. Ma, A. Mohammadzadeh, H. Turabieh, M. Mafarja, S. S. Band, and A. Mosavi, "Optimal type-3 fuzzy system for solving singular multi-pantograph equations," *IEEE Access*, vol. 8, pp. 225692–225702, 2020, doi: 10.1109/ACCESS.2020.3044548.

[42] R. H. Vafaie, A. Mohammadzadeh, and M. J. Piran, "A new type-3 fuzzy predictive controller for MEMS gyroscopes," *Nonlinear Dyn.*, vol. 106, no. 1, pp. 381–403, Sep. 2021, doi: 10.1007/s11071-021-06830-4.

[43] P. N. M. Dorantes and G. M. Mendez, "Non-iterative Wagner–Hagras general type-2 Mamdani singleton fuzzy logic system optimized by central composite design in quality assurance by image processing," in *Recent Trends on Type-2 Fuzzy Logic Systems: Theory, Methodology and Applications*, vol. 425. Berlin, Germany: Springer, 2023.

[44] P. Melin and O. Castillo, "An intelligent hybrid approach for industrial quality control combining neural networks, fuzzy logic and fractal theory," *Inf. Sci.*, vol. 177, no. 7, pp. 1543–1557, Apr. 2007, doi: 10.1016/j.ins.2006.07.022.

[45] S. Safarzadegan Gilan, M. H. Sebt, and V. Shahhosseini, "Computing with words for hierarchical competency based selection of personnel in construction companies," *Appl. Soft Comput.*, vol. 12, no. 2, pp. 860–871, Feb. 2012, doi: 10.1016/j.asoc.2011.10.004.

[46] H. Shahparast and E. G. Mansoori, "Developing an online general type-2 fuzzy classifier using evolving type-1 rules," *Int. J. Approx. Reasoning*, vol. 113, pp. 336–353, Oct. 2019, doi: 10.1016/j.ijar.2019.07.011.

[47] L. I. Cheng-Dong, G. Q. Zhang, W. A. N. G. Hui-Dong, and E. N. Wei-Na, "Properties and data-driven design of perceptual reasoning method based linguistic dynamic systems," *Acta Autom. Sinica*, vol. 40, no. 10, pp. 2221–2232, 2014, doi: 10.1016/S1874-1029(14)60360-8.

[48] K. Mittal, A. Jain, K. S. Vaisla, O. Castillo, and J. Kacprzyk, "A comprehensive review on type 2 fuzzy logic applications: Past, present and future," *Eng. Appl. Artif. Intell.*, vol. 95, Oct. 2020, Art. no. 103916, doi: 10.1016/j.engappai.2020.103916.

[49] A. A. Ibrahim, H.-B. Zhou, S.-X. Tan, C.-L. Zhang, and J.-A. Duan, "Regulated Kalman filter based training of an interval type-2 fuzzy system and its evaluation," *Eng. Appl. Artif. Intell.*, vol. 95, Oct. 2020, Art. no. 103867, doi: 10.1016/j.engappai.2020.103867.

[50] M. A. Balootaki, H. Rahmani, H. Moeinkhah, and A. Mohammadzadeh, "On the synchronization and stabilization of fractional-order chaotic systems: Recent advances and future perspectives," *Phys. A, Stat. Mech. Appl.*, vol. 551, Aug. 2020, Art. no. 124203, doi: 10.1016/j.physa.2020.124203.

[51] E. Ontiveros, P. Melin, and O. Castillo, "High order α-planes integration: A new approach to computational cost reduction of general type-2 fuzzy systems," *Eng. Appl. Artif. Intell.*, vol. 74, pp. 186–197, Sep. 2018, doi: 10.1016/j.engappai.2018.06.013.

[52] D. Wu and J. Mendel, "Recommendations on designing practical interval type-2 fuzzy systems," *Eng. Appl. Artif. Intell.*, vol. 85, pp. 182–193, Oct. 2019, doi: 10.1016/j.engappai.2019.06.012.

[53] F. Chiclana and S.-M. Zhou, "Type-reduction of general type-2 fuzzy sets: The type-1 OWA approach," *Int. J. Intell. Syst.*, vol. 28, no. 5, pp. 505–522, May 2013, doi: 10.1002/int.21588.

[54] W.-H.-R. Jeng, C.-Y. Yeh, and S.-J. Lee, "General type-2 fuzzy neural network with hybrid learning for function approximation," in *Proc. IEEE Int. Conf. Fuzzy Syst.*, Aug. 2009, pp. 1534–1539, doi: 10.1109/FUZZY.2009.5277250.

[55] J. C. Figueroa-García, H. Román-Flores, and Y. Chalco-Cano, "Type–reduction of interval type–2 fuzzy numbers via the Chebyshev inequality," *Fuzzy Sets Syst.*, vol. 435, pp. 164–180, May 2022, doi: 10.1016/j.fss.2021.04.014.

[56] J. Aisbett, J. T. Rickard, and D. Morgenthaler, "Intersection and union of type-n fuzzy sets," in *Proc. Int. Conf. Fuzzy Syst.*, Jul. 2010, pp. 1–8, doi: 10.1109/FUZZY.2010.5584174.

[57] I. B. Türkşen, "From type 1 to full type *n* fuzzy system models," *J. Multiple-Valued Logic Soft Comput.*, vol. 22, nos. 4–6, pp. 543–560, 2014.

[58] P. Fisher, T. Cheng, and J. Wood, "Higher order vagueness in geographical information: Empirical geographical population of type *n* fuzzy sets," *GeoInformatica*, vol. 11, no. 3, pp. 311–330, Aug. 2007, doi: 10.1007/s10707-006-0009-5.

[59] I. B. Türkşen, "Type 2 representation and reasoning for CWW," *Fuzzy Set Syst.*, vol. 127, no. 1, pp. 17–36, 2002.

[60] J. M. Mendel, "Uncertain rule-based fuzzy systems," in *Introduction and New Directions*, 2nd ed. Cham, Switzerland: Springer, 2017, doi: 10.1007/978-3-319-51370-6.

[61] J. M. Mendel, "Uncertain rule-based fuzzy systems," in *Introduction and New Directions*, 1st ed. Upper Saddle River, NJ, USA: Prentice-Hall, 2001. [Online]. Available: https://www.amazon.com/-/es/Jerry-Mendel/dp/0130409693

[62] J. M. Mendel, R. I. John, and F. Liu, "Interval type-2 fuzzy logic systems made simple," *IEEE Trans. Fuzzy Syst.*, vol. 14, no. 6, pp. 808–821, Dec. 2006, doi: 10.1109/TFUZZ.2006.879986.

[63] J. M. Mendel, "General type-2 fuzzy logic systems made simple: A tutorial," *IEEE Trans. Fuzzy Syst.*, vol. 22, no. 5, pp. 1162–1182, Oct. 2014, doi: 10.1109/TFUZZ.2013.2286414.

[64] H. Liang, L. Chen, Y. Pan, and H. K. Lam, "Fuzzy-based robust precision consensus tracking for uncertain networked systems with cooperative-antagonistic interactions," *IEEE Trans. Fuzzy Syst.*, vol. 31, no. 4, pp. 1–15, Apr. 2023, doi: 10.1109/TFUZZ.2022.3200730.

[65] Y. Pan, Q. Li, H. Liang, and H.-K. Lam, "A novel mixed control approach for fuzzy systems via membership functions online learning policy," *IEEE Trans. Fuzzy Syst.*, vol. 30, no. 9, pp. 3812–3822, Sep. 2022, doi: 10.1109/TFUZZ.2021.3130201.

[66] Y. Pan, Y. Wu, and H. K. Lam, "Security-based fuzzy control for nonlinear networked control systems with DoS attacks via a resilient event-triggered scheme," *IEEE Trans. Fuzzy Syst.*, vol. 30, no. 10, pp. 4359–4368, Oct. 2022, doi: 10.1109/TFUZZ.2022.3148875.

[67] G. M. Méndez, L. A. Leduc, R. Colás, A. Cavazos, and R. Soto, "Modelling recalescence after stock reduction during hot strip rolling," *Ironmaking Steelmaking*, vol. 33, no. 6, pp. 484–492, Jul. 2013, doi: 10.1179/174328106X114011.

[68] L.-X. Wang, *A Course in Fuzzy Systems and Control*, 1st ed. Upper Saddle River, NJ, USA: Prentice-Hall, 1996.

[69] L.-X. Wang, "Solving fuzzy relational equations through network training," in *Proc. 2nd IEEE Int. Conf. Fuzzy Syst.*, vol. 2, Jun. 1993, pp. 956–960, doi: 10.1109/FUZZY.1993.327385.

[70] G. M. Méndez and M. de los Angeles Hernández, "Hybrid learning mechanism for interval A2–C1 type-2 non-singleton type-2 Takagi–Sugeno–Kang fuzzy logic systems," *Inf. Sci.*, vol. 220, pp. 149–169, Jan. 2013, doi: 10.1016/j.ins.2012.01.024.

G. M. MENDEZ was born in Durango, Mexico, in 1962. He received the B.S. degree in electronics systems engineering from Instituto Tecnológico y de Estudios Superiores de Monterrey, Nuevo León, Mexico, in 1985, the M.B.A. degree from Facultad de Contaduría Pública y Administración, Universidad Autonoma de Nuevo León, Nuevo León, in 1996, and the M.S. and Dr.-Ing. degrees in mechatronics engineering from Centro de Ingeniería y Desarrollo Industrial, Querétaro, Mexico, in 2005. Since February 1986, he has been a Professor with the Electrical and Electronics Engineering Department, Instituto Tecnológico Nacional de México, Campus Nuevo León, Mexico. His research interests include intelligent systems and industrial process automation.

ISMAEL LOPEZ-JUAREZ received the B.Eng. degree in mechanical-electrical engineering from UNAM, Mexico, in 1991, the M.Sc. degree in instrument design and application from The University of Manchester, U.K., in 1996, and the Ph.D. degree in intelligence robotics from Nottingham Trent University, U.K., in 2000. He was the Founder and the Leader of Grupo de Investigaciónen Mecatrónicay Sistemas Inteligentes de Manufactura, CIATEQ A.C., from 2000 to 2006. Currently, he is the Leader of the Intelligent Manufacturing Laboratory and the Principal Researcher with CINVESTAV, Mexico. His research interests include artificial intelligence, advanced manufacturing, and vision systems.

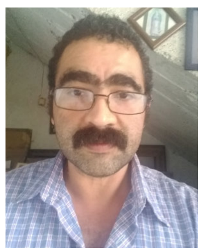

P. N. MONTES-DORANTES was born in Saltillo, Mexico, in 1977. He received the B.S. degree in industrial engineering and systems, the M.S. degree in productivity, and D.Sc. degree in education from Universidad Autónoma del Noreste (UANE) Campus Saltillo, Coahuila, Mexico, in 1999, 2004, and 2021 respectively. Their field of study is the intelligent systems applied in industrial problems and in social sciences. He has works in diverse industrial fields, such as an advisor of metal-mechanic and automotive and work as a Professor with UANE Campus Saltillo on Industrial Engineering and Systems Program, in 2016. His current research interests include the applications of computational intelligence techniques to modeling quality inspection systems, uncertain process modeling, classification problems, and learning methods. He was a member of the Mexican Society of Artificial Intelligence. He is an active member of the Mexican Logistics Association. He is a reviewer of the IEEE TRANSACTIONS ON FUZZY SYSTEMS journal and IEEE LATIN AMERICA TRANSACTIONS journal.

M. A. GARCIA was born in Monterrey, Nuevo León, Mexico, in 1963. She received the B.S., M.S., and Ph.D. degrees in industrial physical engineering from Universidad Autonoma de Nuevo León, Nuevo León, in 2003. Since 1989, she has been a Professor and an Academic Coordinator with Facultad de Matemáticas, Universidad Autonoma de Nuevo León. Her research interests include control process for nonlinear stochastic systems modeling and control, data analysis, and math teaching.